# Variations in Earthquake Detection Across Ocean Networks Canada's Early Warning System

by

Katie McMartin

A Thesis Submitted in Partial Fulfillment of the
Requirements of the

HONOURS PROGRAM

in the School of Earth and Ocean Sciences

Supervisors: Lucinda Leonard and Alireza Mahani


University of Victoria



We acknowledge and respect the Lək̓ʷəŋən (Songhees and Xʷsepsəm/Esquimalt) Peoples on whose territory the university stands, and the Lək̓ʷəŋən and W̱SÁNEĆ Peoples whose historical relationships with the land continue to this day.

# Table of Contents

# List of Figures

# List of Tables

## Acknowledgements

I would like to thank my supervisors Dr. Lucinda Leonard and Dr. Alireza Mahani for taking me on as their Honours student and for their expertise and support over the duration of my research. I would also like to thank Dr. Jesse Hutchinson for his time and assistance attending my honours meetings and offering expertise on Ocean Networks Canada. I would also like to thank Ocean Networks Canada for letting me contribute research to their Earthquake Early Warning system. I would also like to thank my fellow honours students for offering me support as we all learned about conducting meaningful scientific research.

## Abstract

Ocean Networks Canada's Earthquake Early Warning (EEW) system has been in operation since 2023. This system uses P wave parameters measured at onshore and offshore stations to predict strong ground shaking and provide advance warning to operators of infrastructure (e.g., trains, planes) and other subscribers. Since its launch the system has detected hundreds of earthquakes. However, when compared to other organizations, the system is missing events. To investigate, Ocean Networks Canada's earthquake catalog was first compared to those of Natural Resources Canada and the United States Geological Survey. It was found that events are primarily being missed in the northwest and southwest portions of the EEW grid (i.e., in the Explorer plate region south of Haida Gwaii and along the Explorer-Pacific divergent margin) with the system doing a good job of detecting events near Vancouver Island and the Nootka fault zone. In order to determine if events are going undetected because of station geometry (i.e., not enough stations are close enough to the epicentre for P waves to be detected), modelling using ground motion prediction equations was carried out to estimate the minimum detectable magnitude across the grid. In addition, a case study was investigated on a significant undetected event to assess the role of other aspects of the EEW detection algorithm (e.g., epicentre determination). The results showed that the likely reason events are going undetected across the EEW grid is a combination of the geometry of the stations and other aspects of the detection algorithm. The addition of stations from nearby networks (e.g., in Haida Gwaii) and improvements to the epicentre determination algorithm would increase the detection of events across the Ocean Networks Canada Earthquake Early Warning system.

# 1.0 Introduction

Earthquake early warning (EEW) systems are an important measure in response to strong ground shaking offering warning time for infrastructure operators and other subscribers to reduce critical impacts. EEW systems are in operation across the globe, most notably in Japan, Mexico, and the United States. The Mexican Seismic Alert System (SASMEX) has been in operation since 1993; as of 2017 it had detected 6896 earthquakes and issued 158 early warnings (Suárez et al., 2018). Japan has a number of successful earthquake early warning systems operated by the Japan Meteorological Agency (JMA); one of their systems, the Urgent Earthquake Detection and Alarm System (UrEDAS), is able to send out an alert within 1 second after detection of an event (Nakamura & Saita, 2007). Another example is ShakeAlert, which is operated by the United States Geological Survey and supplies warnings to California, Washington, and Oregon. Following improvements to the initial system, ShakeAlert has successfully sent out warnings for a number of M6 events (McGuire et al., 2025). These three examples, and many more, prove that earthquake early warning systems are a great way to mitigate the effects of strong ground shaking.

Southwestern British Columbia is within a seismically active area which has the potential to produce large (M>8) earthquakes, as it has in the past (Clague, 1997; Leonard et al., 2004). Smaller, but still significant, (M6-M7) events have also caused damage on Vancouver Island (Cassidy et al., 2010). The potential for significant ground shaking exemplifies the importance of enabling mitigative actions via an Earthquake Early Warning System like those in operation in Japan, Mexico, and the United States.

In 2015, Ocean Networks Canada (ONC) began developing an Earthquake Early Warning System for southwestern British Columbia which comprises both onshore and offshore stations. In 2019, the system completed its initial stage and it has been in operation since 2023. This system provides advance warning, using several algorithms, for potential catastrophic earthquakes, allowing for mitigative actions prior to the onset of strong shaking. Even though the system has detected hundreds of earthquakes since 2023, the system has missed earthquakes when compared to other organizations; the missed detections are the main focus of this research thesis.

The main questions addressed in this study include: (1) where are events being missed, (2) why are events being missed, and (3) how could the system possibly be improved? Research

involved first comparing the catalogs of ONC, Natural Resources Canada (NRCAN), and the United States Geological Survey (USGS) to determine where earthquakes are being missed. Investigating why earthquakes are being missed is the main portion of this study, in which two possibilities were assessed. Are the earthquakes being missed because of the geometry of the stations (i.e., not enough stations are close enough to the epicentre to record a large enough signal) or is another issue in the earthquake detection algorithm causing events to go undetected? The study involved modelling the minimum detectable earthquake magnitude across the ONC EEW grid area, and comparing the resultant threshold values with the magnitude of missed ONC events to assess if the issue is the geometry of the stations. As well, an investigation into a missed event case study was conducted to assess the possibility that missed detections may result from another issue in the earthquake detection algorithm. Finally, the conclusion of this thesis outlines recommendations for further research that could be conducted, and offers suggestions for improving the earthquake detection capabilities of the ONC EEW system.

# 2.0 Background

## *2.1 Tectonic Setting and Historic Seismicity*

Southwestern British Columbia is in a seismically active area where the Juan de Fuca plate is subducting to the northeast underneath the North American plate at the Cascadia subduction zone (Figure 2.1.1). North of the Juan de Fuca plate is the Explorer microplate; their shared boundary is the Nootka fault zone that hosts left-lateral relative motion (Clague, 1997; Hutchinson et al., 2023). To the west, the Juan de Fuca and Explorer plates are diverging from the Pacific plate along a mid-ocean ridge system segmented by transform faults. To the northwest, there is dominantly transform relative motion (with some convergence) between the Pacific and North America plates offshore Haida Gwaii; the Queen Charlotte fault is the transform boundary.

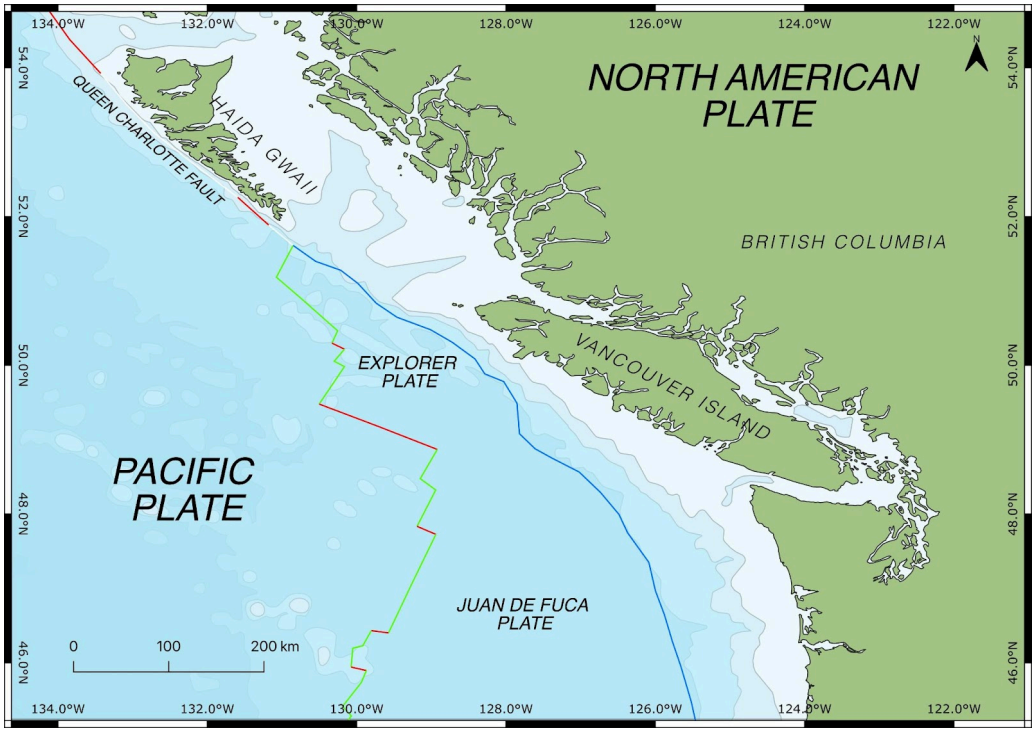


Figure 2.1.1. Map showing the tectonic setting of Vancouver Island. The blue line represents the Cascadia subduction zone, red line shows transform boundaries, and green line shows spreading ridges. Bathymetry and coastline are from Natural Earth (https://www.naturalearthdata.com/downloads/10m-physical-vectors/10m-bathymetry/); tectonic boundaries are from the USGS (www.usgs.gov).

The Cascadia subduction zone is characterized by a lack of instrumentally recorded seismicity, but is well known for its potential to host great (M>8) megathrust earthquakes, with a long geological record of past events (Clague et al., 2000; Bostock et al., 2019). A future earthquake of this magnitude will have catastrophic consequences for residents of coastal BC. Figure 2.1.2 shows the modelled ground motions in a scenario developed by NRCAN that simulates a full rupture (M9.0) of the Cascadia subduction zone megathrust fault. The peak ground acceleration resulting from the simulated epicentre around Victoria would be 22 %g.

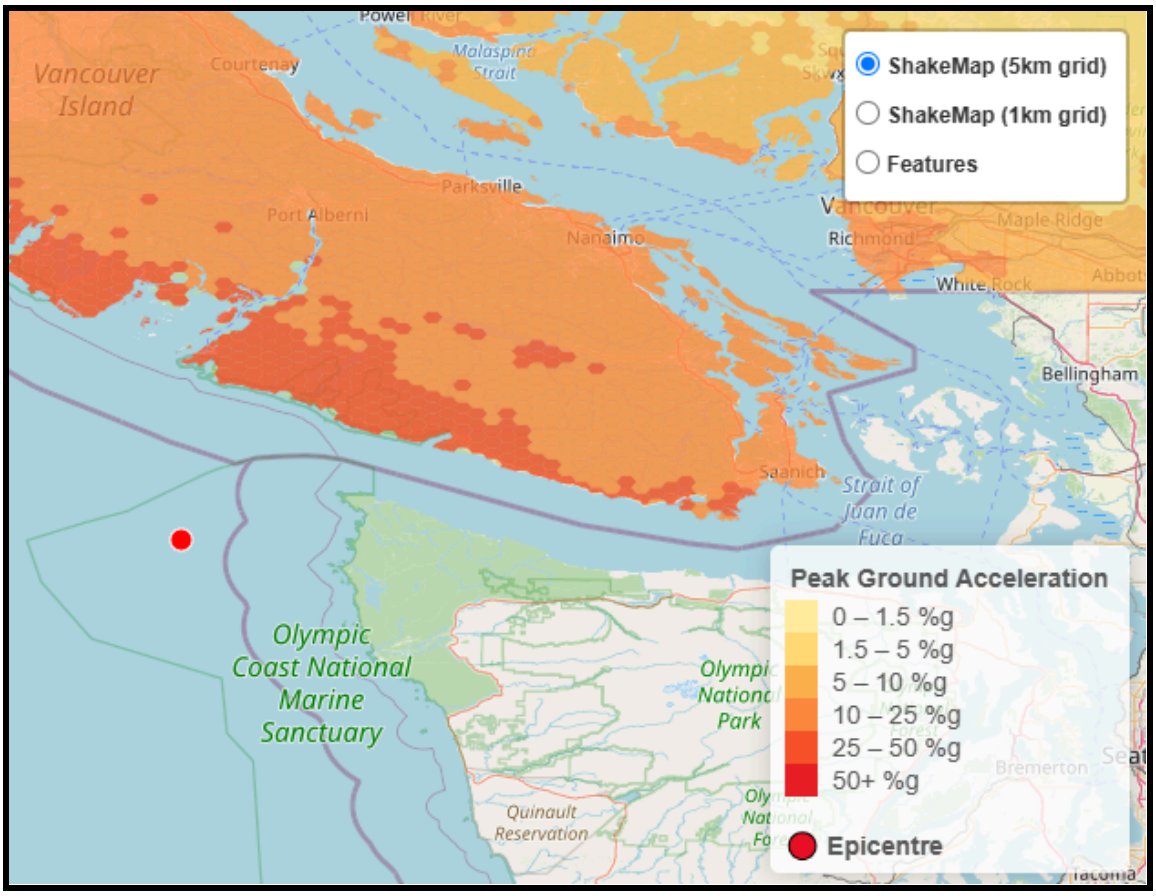


Figure 2.1.2. Simulated scenario of M9.0 full rupture of the Cascadia subduction zone megathrust. Shown on the map is southern Vancouver Island with the offshore scenario epicentre shown by the red dot. Colours represent peak ground acceleration in units of percentage of the acceleration of gravity. This simulation was done by Natural Resources Canada and was screenshot from riskprofiler.ca.

The last megathrust earthquake occurred on the evening of January 26, 1700. The evidence of this event is supported by a so-called “orphan” tsunami that impacted Japan, with timing that matches the oral history of coastal Indigenous peoples that reports an event with widespread strong shaking and flooding, as well as geological records of sudden coastal subsidence, death of submerged coastal trees, and offshore turbidity currents (e.g., Clague, 1997; Leonard et al. 2004). The average interval between events has been estimated to be approximately 500 years; however, there is uncertainty in this statement because we are relying on preserved geological records which might not represent the number of actual events that have occurred (Atwater et al., 1995; Clague 1997).

The Cascadia subduction zone region generally has lower-level (up to M4-M6) seismicity (Figure 2.1.3, Babaie Mahani et al., 2024). Figure 2.1.3 shows that seismicity is concentrated

around the divergent and transform boundaries between the Pacific and Explorer plates. However, the region offshore Vancouver Island does host M>6 earthquakes (e.g., M 6.5 September 15, 2024, south of Haida Gwaii) on a much more regular basis than megathrust earthquakes. An event of this magnitude closer to densely populated areas is also of concern. Figure 2.1.4 shows a simulated M7.3 rupture of the Leech River fault developed by NRCAN. The map shows modelled peak ground acceleration in Greater Victoria and Sooke resulting from this hypothetical earthquake. The predicted ground acceleration in the area of Esquimalt is greater than 50 %g. This simulated event shows that while a M9.0 megathrust event is of high seismic concern, so are lower-magnitude earthquakes, like a M7.3 rupture of the Leech River fault, that occur much closer to large population centres. Recent events have occurred near Vancouver Island with moderate ground shaking resulting in damage, such as the 1943 M7.3 crustal event and the 2001 M6.8 Nisqually Juan de Fuca slab earthquake (Cassidy et al. 2010).

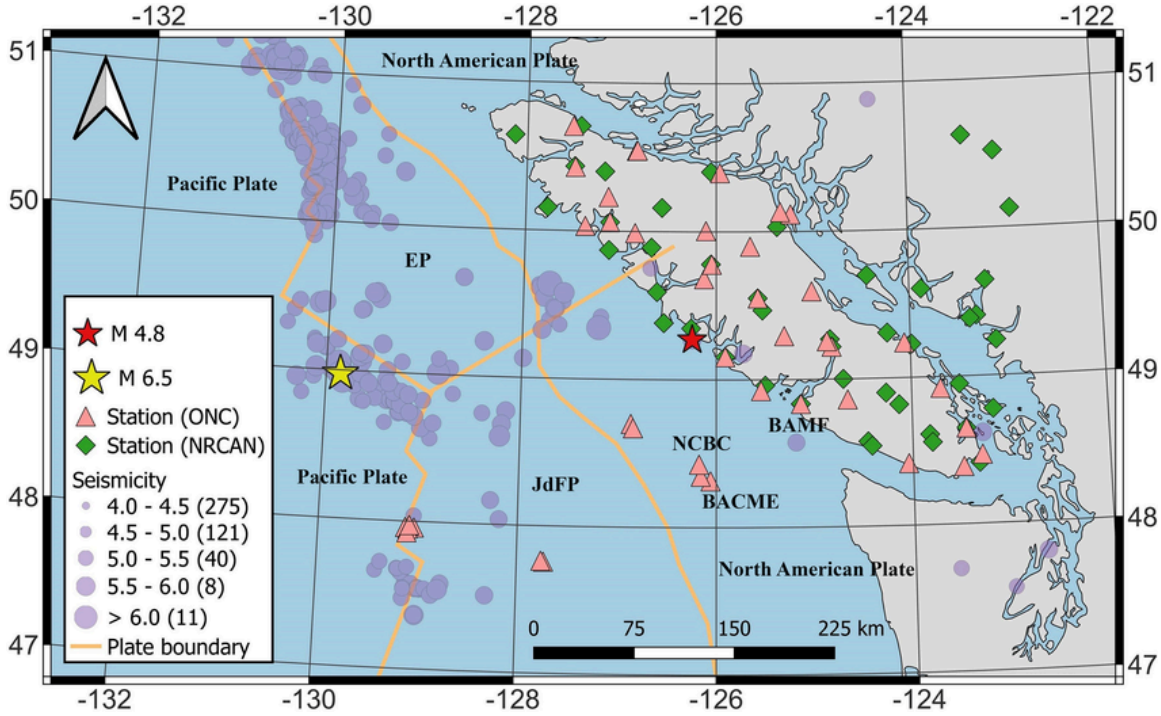


Figure 2.1.3. Map of the seismicity of southwestern British Columbia gathered from data from ONC and NRCAN including stations from ONC and NRCAN. EP and JdFP are the tectonic plates Explorer Plate and Juan de Fuca Plate respectively. BAMF (Bamfield station), NCBC (Barkley Canyon Upper Slope South station), and BACME (Barkley Canyon Mid-East station) are all offshore stations. Map from Babaie Mahani et al. (2024)

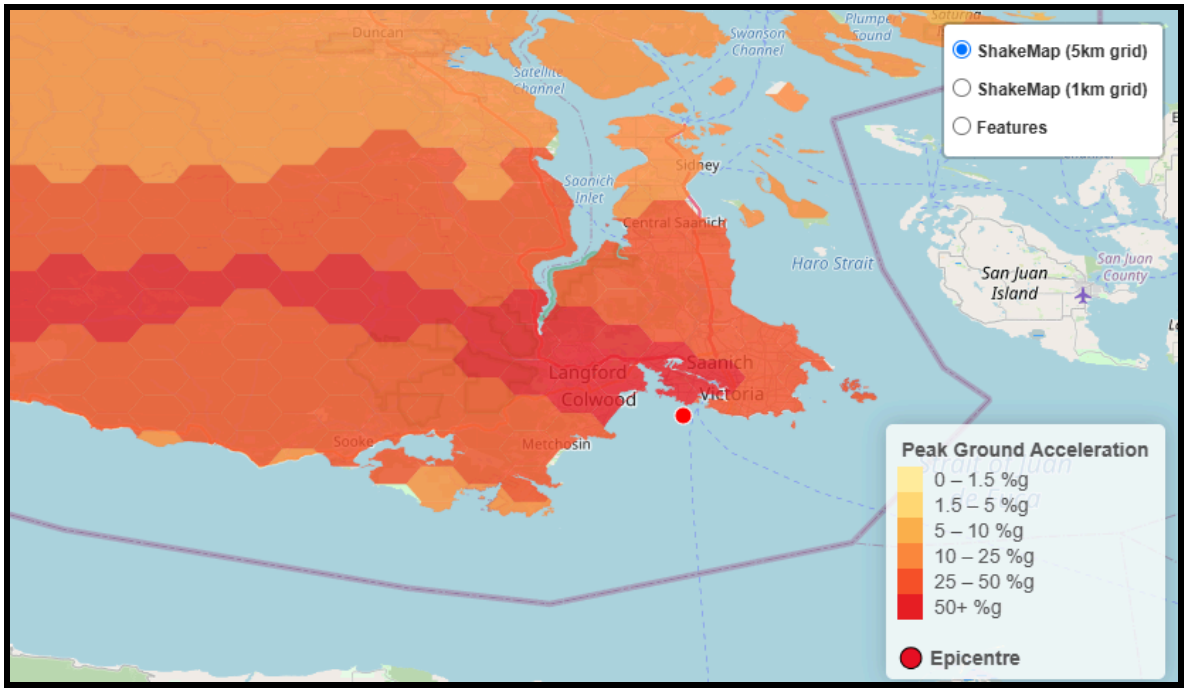


Figure 2.1.4. Simulated scenario of M7.3 rupture of the Leech River Fault. Shown on the map is Greater Victoria and Sooke with the scenario epicentre shown by the red dot. Colours represent peak ground acceleration in units of percentage of the acceleration of gravity. This simulation was done by Natural Resources Canada and was screenshot from riskprofiler.ca.

## *2.2 Earthquake Early Warning Systems*

EEW systems are based on the principle of providing enough warning such that recipients, including infrastructure operators, have enough time for mitigation efforts (e.g., preventing planes from landing, shutting down trains, preventing traffic from entering tunnels) before damaging seismic waves arrive. These damaging seismic waves are the secondary (or shear) waves and surface waves which always follow the generally non-damaging primary waves (called primary because they arrive first). Primary waves (P waves) are compressional waves and cause particle motion that is parallel to the wave propagation direction, whereas secondary waves (called secondary because they arrive second, AKA S waves) cause particle motion perpendicularly to wave propagation (Figure 2.2.1). These two waves are the basis of different EEW systems, but P waves are important for modern systems.

Surface waves are the seismic waves that cause the most damage. These waves are generated at an interface such as the Earth's surface, when energy from P- and S- waves is converted to different types of waves that propagate along the surface. These waves are called Rayleigh waves and Love waves (Figure 2.2.1). The level of ground shaking caused by surface

waves and/or S waves are what an Earthquake Early Warning system aims to predict, to enable mitigative actions.

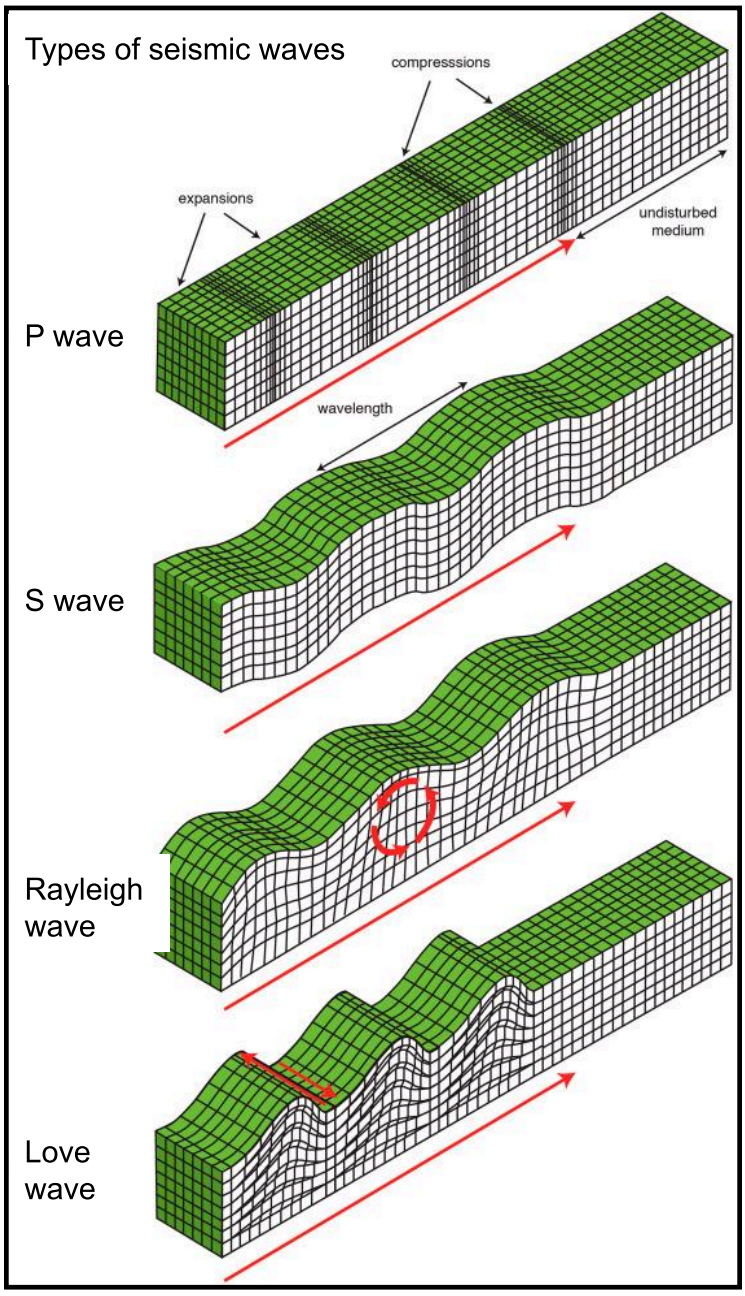


Figure 2.2.1. Image showing types of seismic waves; P wave, S wave, Rayleigh wave, and Love wave. Shown is the direction of propagation (red arrow) as well as how each of the seismic waves move material as it propagates through. This image is from Hersir et al. (2022).

There are three main types of EEW systems: front detection system, network method, and on-site method (Hoshiba, 2013; Cremen & Galasso, 2020). The front detection system has

stations set up between the source and target and sends a warning once the S wave has reached at least one of these stations; this type of system is not generally used anymore. The network method and on-site method are based on the arrival of P waves and provide more warning time. The on-site method relies on one station of a network of stations, detecting and evaluating P-wave parameters to predict peak ground motion and send out an alert. The network method, on the other hand, requires data from multiple stations in the network in order to evaluate P-wave information (Hoshiba, 2013). The benefit of a network system is that there are fewer false alarms because of the multiple station requirement; this however can be an issue with the on-site method. However, the on-site method can deliver faster alerts because only one station is required to send an alert (Cremen & Galasso, 2020).

### *2.3 Ocean Networks Canada's Early Earthquake Warning System*

The ONC EEW system uses the network system method with both onshore and offshore stations. The offshore stations are seafloor seismic instruments that are a part of NEPTUNE's (North-East Pacific Time-series Undersea Networked Experiments) cable network which expands across the Cascadia subduction zone. The addition of offshore sensors from NEPTUNE increases the accuracy of the system, particularly for offshore earthquakes and provides more warning time (Schlesinger et al., 2021).

ONC's EEW system covers a grid from 46 to 52.2 °N and -131.75 to -122 °W. The system operates with the basic process: earthquake parameters are collected and measured at an accelerometer station and/or Global Navigation Satellite Systems (GNSS) receiver; for onshore sites this is done on site, whereas for offshore stations (which have accelerometers, but no GNSS) this is done by sending waveforms onshore for the assessment of parameters.

#### *2.3.1 ONC EEW Magnitude Algorithms*

The ONC algorithm calculates three magnitude values based on data from accelerometers and GNSS receivers. $M_{Pd}$ (equation 1.1) is calculated by P wave displacement ($P_d$) using the vertical component of acceleration time series. $M_{PD}$ (equation 1.2) is calculated by using P wave displacement ($P_D$) using horizontal components of acceleration and GNSS time series. $M_{PGD}$ (equation 1.3) which is similar to $M_{PD}$ but instead uses two horizontal components and one vertical for measurement of P wave displacement ($P_{GD}$). If the $M_{Pd}$ is above 6.0, the system will

consider $M_{PGD}$ and then $M_{PD}$ and will revert to $M_{Pd}$ if these two do not exist. If the event is M<6 then the $M_{Pd}$ is used. R in the equations 1.1-1.3 is the distance in km.

$$M_{Pd} = 1.23(\log_{10}P_{di}) + 1.38(\log_{10}R_i) + 5.39 \quad [1.1]$$

$$M_{PD} = \frac{log_{10}P_D + 0.893 + 1.73\ log_{10}R}{0.562} \quad [1.2]$$

$$M_{PGD} = \frac{log_{10}P_{GD} + 5.013}{1.219 - 0.178log_{10}R} \quad [1.3]$$

*2.3.2 ONC EEW Epicentre Location Algorithms*

Two different methods are used to determine epicentre location. Direct Grid Search (DGS) requires at least 4 stations detected within 120 s to register the P wave (i.e., the P-wave arrival being 5 times larger than the background noise at the station) and assumes a depth of 25 km. The DGS algorithm uses an established grid (46 to 52.2 °N and -131.75 to -122 °W, 0.15° by 0.15°); each point on this grid is determined to be a potential source location. DGS uses time differences of arrivals (TDOA; which in this case would be time difference of P-wave arrivals) between two stations and the hyperbolic intersection forward problem (equation 2.1) to estimate the approximate epicentre location. The hyperbolic intersection forward problem equation is calculated by using the time ($t_{si}$ and $t_{sj}$) between potential source location (s) and each station (i, j) and the TDOA between the two stations ($\delta t_{ij}$). $t_{si}$ and $t_{sj}$ are calculated using an assumed velocity and calculating distance between source and location. w is a parameter which takes into account uncertainties in travel-time and arrival time differences. Equation 2.1 is then calculated at each grid point for every possible 2 stations configuration. The values ($P(s)_{ij}$) at each grid point are then summed to obtain the maximum likelihood estimate which is the approximate epicentre location. This method remains strong in the presence of errors (Schlesinger et al., 2021).

$$P(s)_{ij} = exp(-\frac{1}{w}(t_{si} - t_{sj} - \delta t_{ij})^2) \quad [2.1]$$

The second method, Linear Least Squares (LLS), is based on work by Gillette and Silverman (2008) and also requires at least 4 stations. This method calculates the epicentre in one single step by solving a set of linear equations. The algorithm picks two stations from the initial four and uses TDOA parameters to solve the system of equations to get the approximate coordinates of the epicentre. The issue with this system is that small errors in the input can cause large errors in the resulting epicentre determination (Schlesinger et al., 2021).

# 3.0 Methods

## *3.1 Analysis of the Ocean Networks Canada Catalog*

Used in this study are earthquake event catalogs from three organizations; NRCAN, the USGS and ONC. The events in these catalogs are within the ONC grid (46 to 52.2 °N and -131.75 to -122 °W). The data obtained from this catalog are used to assess the areas within the ONC grid where the EEW system is missing or differently recording earthquakes compared to NRCAN and the USGS. In this case, the focus of comparison is mostly between NRCAN and ONC, since NRCAN has access to more local stations than the USGS and has a more complete and accurate catalog for the region.

Information from the ONC catalog was accessed through an ONC-approved ticket to create a file readable in MATLAB. Code was then created to access all necessary information: magnitude, event ID number, time, latitude/longitude of event, and the organization the event was recorded by. The catalog organizes the earthquakes by two ID numbers: the event ID which is a shared identifier that links the same earthquake events across multiple organizations (ONC, USGS, NRCAN) and the detailed ID, a unique identifier assigned to each individual recording of an event by a specific organization. Thus a single event could have up to four ID numbers if recorded by all three organizations.

The finalized data were plotted in QGIS for visualization, along with the locations of active and inactive stations as of January 17, 2025, as provided by Dr. Jesse Hutchinson (Figure 3.1). A visual comparison of events recorded by the three organizations was then made, to identify where the ONC system has missed earthquakes or differently recorded earthquakes, compared to NRCAN and the USGS.

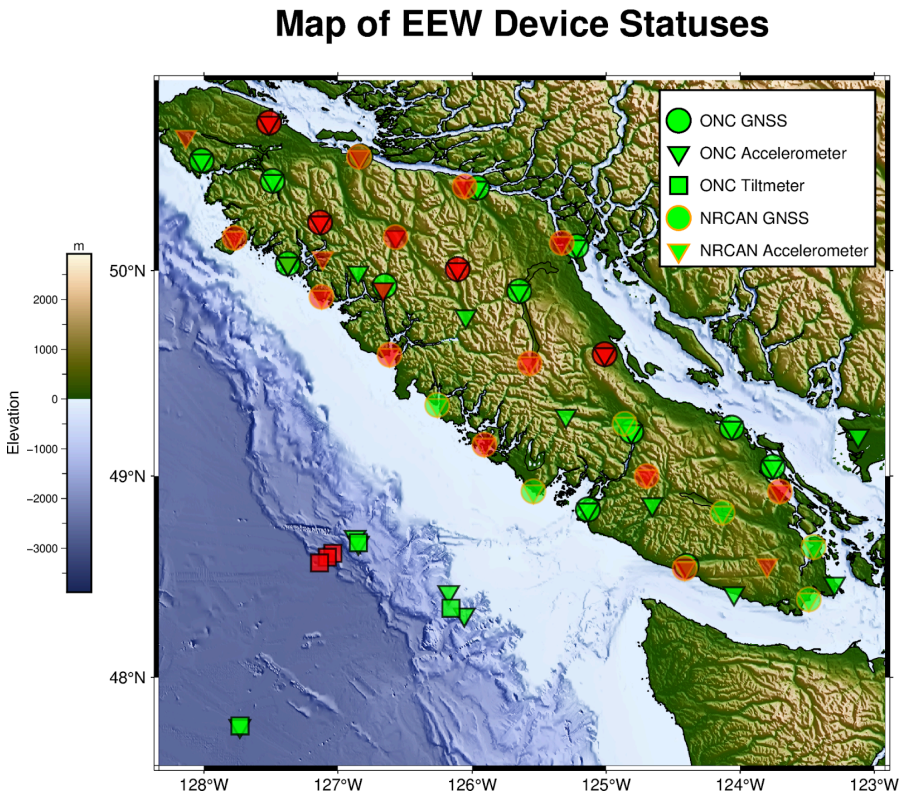


Figure 3.1. Map shows the locations of active Ocean Networks Canada (ONC) EEW network stations in green as of January 17, 2025 when this map was produced by Dr. Jesse Hutchinson. Red-filled symbols are network stations that were inactive on this date. The circles denote the stations that are GNSS stations, triangles are GNSS accelerometers, and squares are tiltmeters which are not used in this analysis. The shapes outlined in black are ONC stations and the shapes outlined in red are NRCAN stations.

### *3.2 Atkinson (2005) Ground Motion Prediction Equation*

The function of a ground motion prediction equation (GMPE) is to use parameters of magnitude, type of event, and distance from an earthquake epicentre to predict the peak seismic wave amplitude at a specific location. For this study, the GMPE chosen was determined by Atkinson (2005), and is a set of equations applicable to the Cascadia subduction zone region (crustal, offshore, in-slab, and transition), to calculate amplitude (peak ground motion acceleration) for earthquakes of magnitude 3.0-6.0 at a range of distances. Equations 3-5 are used in this analysis to predict maximum acceleration at short ($R_{ij} \leq r_{t1}$), intermediate ( $r_{t1} < R_{ij} \leq r_{t2}$ ), and long ($R_{ij} > r_{t2}$) distances. For crustal events, $r_{t1}$ is 90km and $r_{t2}$ is 300 km, defining which Equation (3-5) will be used depending on the size of $R_{ij}$ compared to $r_{t1}$ and $r_{t2}$. These parameters are different for the different event locations. $R_{ij}$ is the distance from the earthquake i epicentre to the station j.

$$\mathbf{R_{ij} \leq r_{t1}} \quad [3]$$

$$\log A_{ij} = c_i + c_2 (M_i - 4) + c_3 (M_i - 4)^2 + b \log R_{ij} + c_4 R_{ij}$$

$$\mathbf{r_{t1} < R_{ij} \leq r_{t2}} \quad [4]$$

$$\log A_{ij} = c_1 + c_2 (M_i - 4) + c_3 (M_i - 4)^2 + b \log r_{t1} + t \log(R_{ij}/r_{t1}) + c_4 R_{ij}$$

$$\mathbf{R_{ij} > r_{t2}} \quad [5]$$

$$\log A_{ij} = c_1 + c_2 (M_i - 4) + c_3 (M_i - 4)^2 + b \log r_{t1} + t \log(r_{t2}/r_{t1}) - 0.5 \log(R_{ij}/r_{t2}) + c_4 R_{ij}$$

In the equations, $M_i$ is the magnitude of earthquake i. $A_{ij}$ is the acceleration from earthquake event i that occurs at station j. $b$ is the geometric spreading coefficient and $c_1$ through $c_4$ are other coefficients.

Atkinson (2005) provides four tables of parameters for coefficients $b$ and $c_1$-$c_4$ depending on the region of Cascadia being analyzed: crustal, offshore, in-slab, and transition. For simplicity, in this analysis the offshore parameters were used, since most earthquakes in the catalog are offshore; these are outlined in Table 1.

Table 1. Coefficients for offshore scenario earthquakes for use in Equations 3-5

| f | c1 | c2 | c3 | b | t | c4 | rt1 | rt2 |
|---|---|---|---|---|---|---|---|---|
| 1 Hz | -0.881 | 1.479 | -0.187 | -0.338 | -1.92 | -0.0018 | 140 km | 260 km |

### *3.3 Modeling Using the Ground Motion Prediction Equation*

The method used to model the magnitude detection threshold of the ONC grid is based on the method used in Babaie Mahani et al. (2016). All the following modelling was done in MATLAB. The ONC EEW grid was first created; the extent of the system currently is from a latitude of 46.0 to 52.2 degrees North and a longitude of -131.75 to -122.0 degrees East. The spacing used for this grid was 0.1 degrees which created 5544 grid points. The latitude and longitude of stations active on January 17, 2025 (28 stations) were also added to the model as a representation of the active stations on a given day. Only stations that are accelerometers, or that comprise both accelerometers and GNSS instruments, were included in this study; thus tiltmeter stations were removed. Then, station-grid point pairings were created, and the distance (in km) from each point on the grid to each station was calculated.

For coding efficiency, acceleration was calculated across an array of distances of 1-1000 km with 0.1 km increments and an array of earthquake magnitudes from 3.0 to 6.0 with 0.2

increments. This created a 2D matrix of acceleration values for 9991 distances and 16 different magnitudes. Code was then created to associate the distance calculated between the station-point pairings and the 2D acceleration matrix across the 16 different magnitudes (i.e., if the distance between station and grid point is 678.1 km, then the code would choose the acceleration in the 2D matrix where the distance was 678.1 km and would store this value for each magnitude). This resulted in a 3D matrix of 5544 grid points across 28 stations evaluated at 16 different magnitudes.

Background noise at most stations was provided by Dr. Alireza Babaie Mahani (Table 2). The table shows the stations used in this background noise study. PSD refers to power spectral density and is given in units of $m/s^2$, which was then converted to $cm/s^2$. An average of the offshore and onshore station background noise (in $cm/s^2$) was used for the signal to noise ratio calculations. An initial signal to noise ratio (SNR) of 5 is established, which is similar to the SNR threshold for event detection at stations in the ONC EEW system. The code written to evaluate SNR will label each point in the 3D matrix as being above the SNR (label = 1) or below/equal to the SNR (label = 0).

The main priority of this study is to establish magnitude detection thresholds across the ONC grid. For an earthquake to be identified by the ONC EEW system, 4 stations are required to detect the event. The 3D matrix has associated values (0 or 1) for all 5544 grid points across 28 stations and 16 magnitudes. For each station-point pairing, the number of stations detecting the earthquake acceleration (label = 1) are added up for each of the 16 magnitude values. Code was written to choose which of the 16 magnitudes had a number of stations greater than or equal to 4. Then a table of minimum detectable magnitude for each grid point was created. Initial maps of the result of this modelling were completed in QGIS.

### *3.4 Sensitivity Testing of the Detectable Magnitude Model*

Various different sensitivity tests of the system were completed. These included testing the effects of changing the number of active stations, increasing the background noise level, and changing the 4 station association requirement to 3 stations. The resultant minimum detectable magnitude values for each scenario were also mapped using QGIS for comparison. All these sensitivity tests contribute to the interpretations and final recommendations for the ONC EEW system.

Table 2. Seismic background noise at Ocean Networks Canada stations. Station name contains the date range of analysed data; for example, the noise values for NV_AL2H_20220120_20220302 are based on data recorded from January 20, 2022 to March 2, 2022.

| Station | 1 sec (1 Hz) | |
|---|---|---|
| | PSD (m/ss) | PSD (cm/ss) |
| NV_AL2H_20220120_20220302 | 0.0000001 | 0.000010986153642 |
| NV_BAMF_20220201_20220228 | 0.0000002 | 0.000015518354490 |
| NV_BCOV_20220301_20220331 | 0.0000002 | 0.000017411880118 |
| NV_CMBR_20220120_20220302 | 0.0000001 | 0.000010986153642 |
| NV_GLDR_20220201_20220228 | 0.0000002 | 0.000015518354490 |
| NV_PGC5_20220301_20220331 | 0.0000001 | 0.000010986153642 |
| NV_PHRD_20220201_20220228 | 0.0000001 | 0.000013830747997 |
| NV_QISL_20220301_20220331 | 0.0000001 | 0.000010986153642 |
| NV_SC04_20220201_20220228 | 0.0000001 | 0.000012326667128 |
| NV_STRA_20220301_20220331 | 0.0000001 | 0.000010986153642 |
| NV_TAYR_20220301_20220331 | 0.0000001 | 0.000010986153642 |
| NV_TAYR_20230201_20230224 | 0.0000001 | 0.000012326667128 |
| NV_UCLU_20220301_20220331 | 0.0000002 | 0.000024594934389 |
| NV_ZEBA_20220120_20220228 | 0.0000001 | 0.000012326667128 |
| CN_NTKA_20211217_20220118 | 0.0000004 | 0.000038980344082 |
| CN_PGC_20220301_20220330 | 0.0000002 | 0.000021920258347 |

| | | |
|---|---|---|
| NV_BACME_20211217_20220118 | 0.0000025 | 0.000245949343888 |
| NV_CBC27_20211217_20220118 | 0.0000022 | 0.000219202583474 |
| NV_CQS64_20211217_20220118 | 0.0000020 | 0.000195364508162 |
| NV_NC89_20211217_20220118 | 0.0000020 | 0.000195364508162 |
| NV_NCBC_Buried_No_VPS_20220806_20220814 | 0.0000011 | 0.000109861536415 |
| NV_NCBC_Buried_with_VPS_20180901_20181009 | 0.0015518 | 0.155183544896307 |
| NV_NCBC_Not_Buried_No_VPS_20211217_20220118 | 0.0000055 | 0.000550611995179 |

# 4.0 Results

## *4.1 Comparison of Earthquakes Detected by Ocean Networks Canada, Natural Resources Canada, and the United States Geological Survey*

The compiled EEW earthquake catalog from ONC that includes events from ONC, NRCAN, and the USGS is provided in Table A1 (Appendix A). The table lists earthquakes from January 22, 2022 to February 14, 2025, the time period analysed in this study.

Figure 4.1 shows maps of the earthquakes in the catalog, divided into those detected by ONC (part a), NRCAN (part b), and the USGS (part c). Added to this map are two red square boxes in the northwest and southwest where ONC seems to have missed significantly more data when compared to NRCAN and USGS. However, the system appears to have a relatively complete detection on or adjacent to Vancouver Island as well as along the Nootka fault.

For comparison, Figure 4.1(d) shows the missed ONC events (when the ONC catalog is compared to the NRCAN catalog) which are concentrated in the same regions as the two red boxes. There are 271 missed events over a time range from January 2022 to February 2025. The magnitude range of the missed events is 3.5-6.5.

It is important to note that there are differences in the completeness and accuracy of the three catalogs. ONC is expected to have fewer events since it has a smaller station network and lower accuracy of magnitude and epicentre estimation since the focus of this system is on increasing the speed of early warning. Whereas, NRCAN and USGS evaluate longer wave forms for magnitude and epicentre location thus increasing their accuracy. USGS has less earthquakes in comparison to NRCAN because the USGS uses fewer stations in the region.

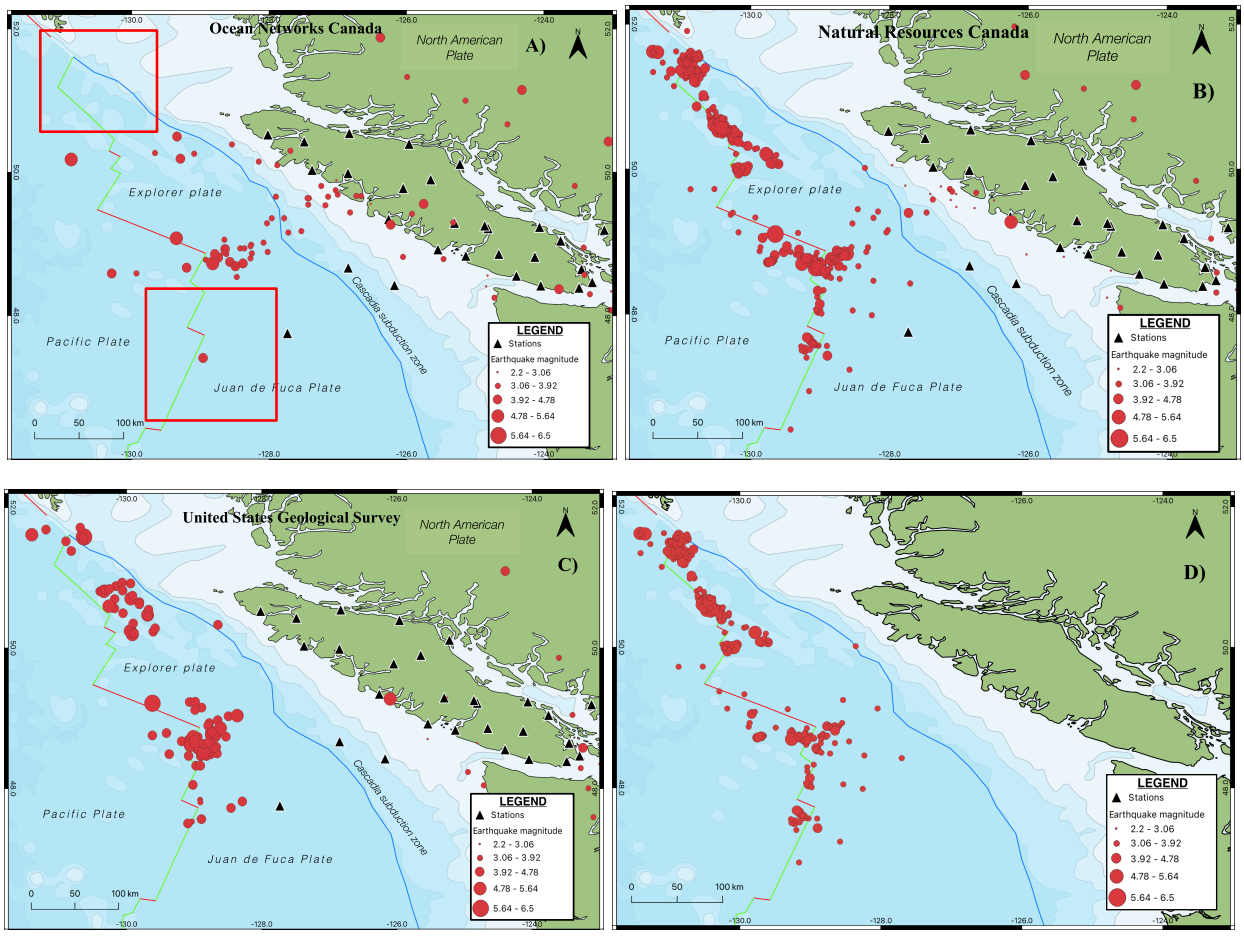


Figure 4.1. Maps showing the epicentres and magnitudes of earthquakes in the ONC EEQ catalog, plotted using QGIS software. Events detected by (a) Ocean Networks Canada, (b) Natural Resources Canada, and (c) the United States Geological Survey. The fourth map (d) shows the missed ONC events (i.e., those detected by NRCAN but not by ONC). The red dots represent earthquake epicentres, scaled by magnitude, and black triangles represent ONC EEW stations. Bathymetric and coastline files were developed by Natural Earth https://www.naturalearthdata.com/downloads/10m-physical-vectors/10m-bathymetry/ tectonic boundaries were developed by USGS www.usgs.gov

### *4.1.1 Case Study September 15, 2024 M6.5 Earthquake*

In analyzing the earthquake detection between organizations there was one significant event that noticeably was not detected by ONC, but is included in the catalogs of both NRCAN and the USGS. NRCAN detected an M 6.5 earthquake on September 15th, 2024 at 15:22:44 PDT, 212 km WSW of Bella Bella, BC, as shown in Figure 4.1.1. It is surprising that the earthquake went undetected by ONC, since an event of this magnitude should be detected by all or by a majority of the stations in the ONC EEW network. Thus, an investigation was warranted, to determine why the event was missed.

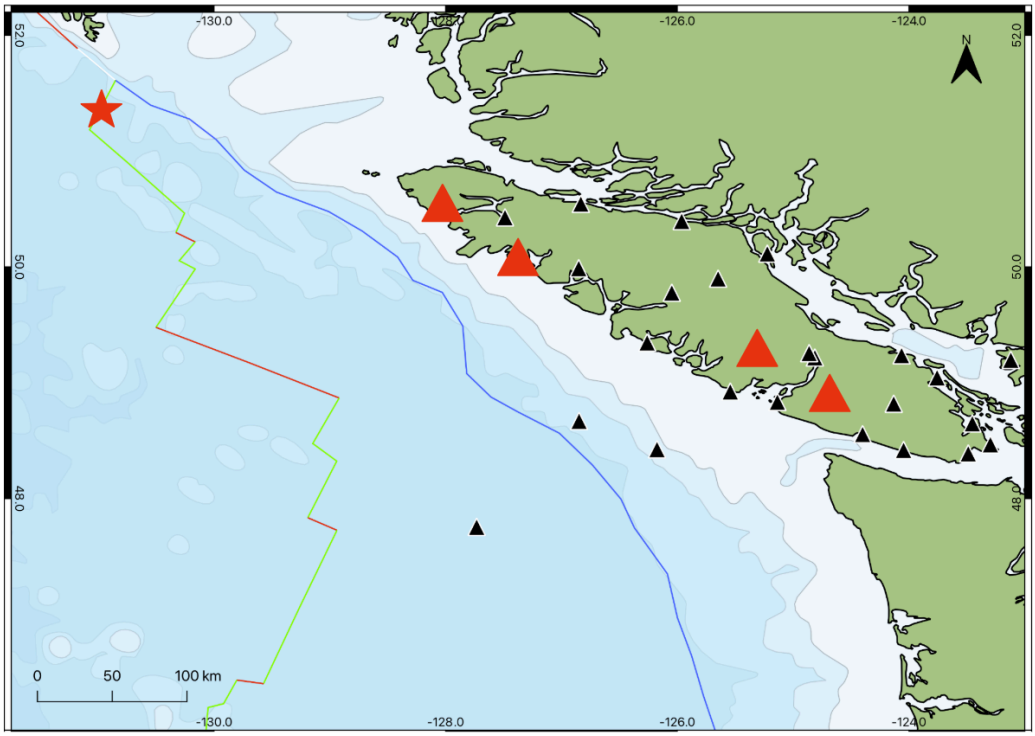


Figure 4.1.1. Map generated in QGIS showing the NRCAN epicentre (red star) of the M6.5 event on September 15th, 2024. Shown are the active stations in the ONC EEW network on January 17, 2025. The red triangles show the location of the 4 stations that detected P waves. Also shown are the plate tectonic boundaries. Tectonic boundaries are from the USGS www.usgs.gov. Bathymetry and coastline are from Natural Earth (https://www.naturalearthdata.com/downloads/10m-physical-vectors/10m-bathymetry/)

Details within the ONC earthquake catalog revealed that a total of 18 ONC EEW stations (Table 3) showed activity of detection, including 4 stations which recorded P wave parameters. These 4 stations met the requirement for event association, and estimated magnitude values as shown in Table 3. Event association is shown in the code as a parameter called “associated”; if this parameter has a value of 1 then the detection at that station is considered valid, but if the value is 0 then the detection is considered not valid. For all 18 ONC station detections for this event, the associated values were 0, meaning none of the detections were considered valid. A possible reason for this is that all 18 stations recorded S-wave arrivals, but 14 stations did not detect P-wave arrivals. Since P-wave detection is essential to the algorithm detecting an event, a lack of P-wave detection would prevent those stations from being associated.

The uncertainty here is why exactly the 4 stations that did record P wave parameters were not associated as an event, thereby enabling the system to register an event detection. After running back the event, there is a hypothesis. The system has two epicentre algorithms (DGS and

LLS, described in section 2) and it has a requirement that the epicentres determined by the two algorithms must be within 80 km of each other, or else the event will be considered invalid. This is the likely reason that the earthquake was considered invalid. Another important observation is that the 4 stations are all in one direction from the event; this could have contributed to the epicentre determination algorithm not accurately locating the event.

Table 3. Details of event detection of September 15, 2024 M6.5 Earthquake at ONC EEW Stations

| **Site Detection**[1] | **Station number** | **Device Type**[2] | **On (1)/off (2) shore** | **Magnitude**[3] |
|---|---|---|---|---|
| 1 | 24318 | 1 | 1 | no |
| 2[4] | 23462 | | | no |
| 3 | 24059 | 1 | 1 | no |
| 4 | 66800 | 1 | 1 | no |
| 5 | 24412 | 1 | 1 | yes (5.5) |
| 6 | 33039 | 1 | 1 | no |
| 7 | 66960 | 1 | 1 | yes (5.3) |
| 8 | 24063 | 1 | 1 | no |
| 9 | 24150 | 3 | 2 | no |
| 10 | 66820 | 1 | 1 | yes (5.9) |
| 11 | 24070 | 1 | 1 | no |
| 12 | 66900 | 1 | 1 | no |
| 13 | 67000 | 1 | 1 | no |
| 14 | 24311 | 1 | 1 | no |
| 15 | 66860 | 2 | 1 | yes (4.4) |
| 16 | 24316 | 2 | 1 | no |
| 17 | 24313 | 1 | 1 | no |
| 18 | 66940 | 2 | 1 | no |

[1] Site detection is numbered as it shows up in the database
[2] The numbers denote the station as being either an accelerometer and GNSS (1), accelerometer (2), or a tiltmeter (3)
[3] This column shows if the magnitude was recorded and if so what magnitude value was recorded.
[4] Note could not find data on what the device type and whether it was onshore or offshore

## *4.2 Ground Motion Modelling*

### *4.2.1 Preliminary Analysis of Ground Motion Prediction Equation Uncertainties*

Prior to modelling with the GMPE, an analysis of the differences between the parameters for different earthquake locations (offshore, crust, in-slab, and transition) was conducted to analyze any uncertainty in using just offshore parameters.

Figure 4.2.1 shows the peak ground acceleration calculated using parameters for the four earthquake location types across a range of distances for earthquake magnitudes of 6, 5, and 3. In each graph, the different peak ground acceleration curves converge to approximately similar values at ~75 km (M3) and ~150 km (M6) and diverge at distances closer. This shows that with increasing magnitude values, the peak ground acceleration diverges to a greater degree closer to the epicentre.

Thus, using just offshore parameters for non-offshore earthquakes creates a relatively low uncertainty at distances greater than ~75 km (M3) and ~150 km (M6) regardless of the magnitude value. However, the uncertainty increases closer to the earthquake epicentre and with increasing magnitude values. This would cause uncertainty in the areas on and around Vancouver Island since an epicentre near the Island would be close to or within the ~75-150 km range, especially for higher magnitude earthquakes.

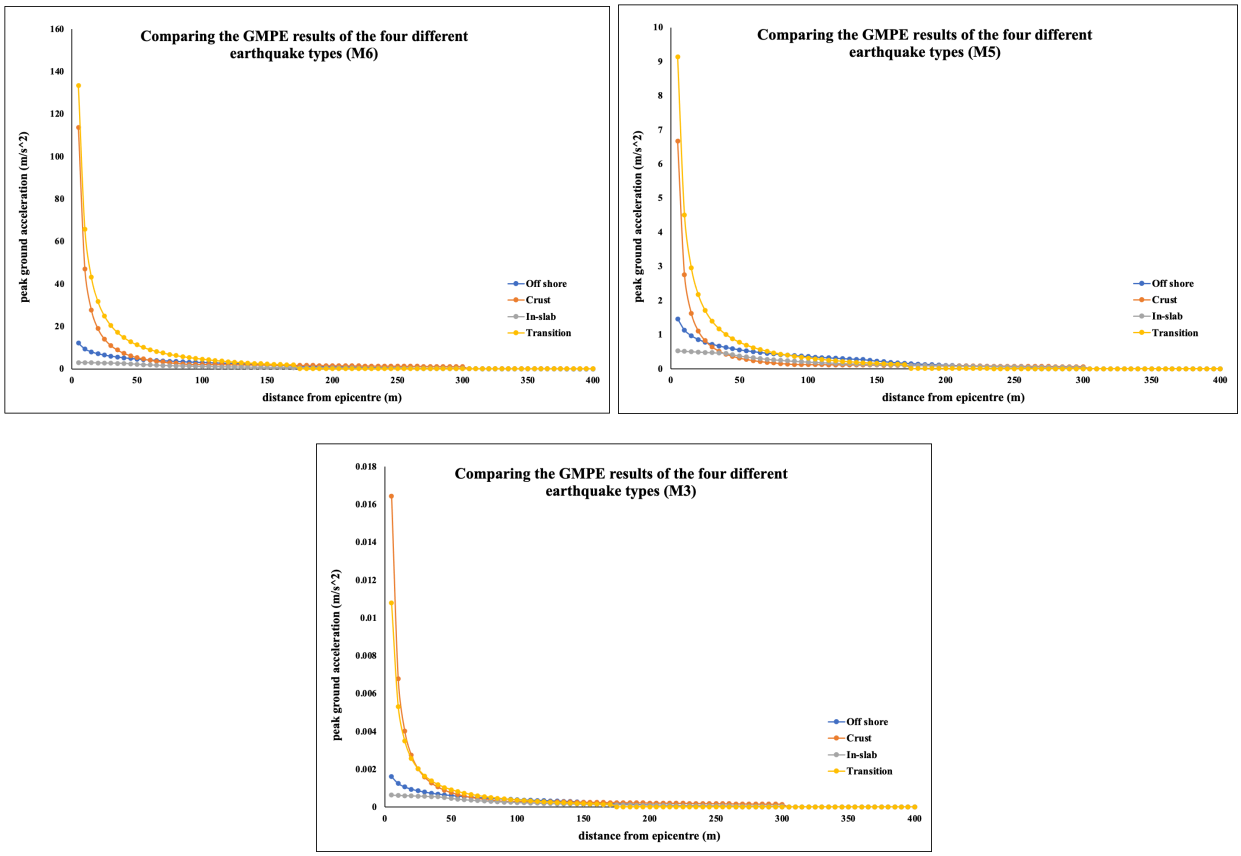


Figure 4.2.1. Peak ground motion acceleration values calculated using Equation 1, with parameters for 4 different earthquake location types across the Cascadia subduction zone. The top left graph shows values for a magnitude 6 earthquake, top right magnitude 5, and bottom magnitude 3. The 4 different lines show the trend of peak ground accelerations across a range of distances for the four different earthquake location types; off shore, crust, in-slab, and transition. The offshore parameters are used throughout this project.

### *4.2.2 Initial Model Results: Estimation of Minimum Detectable Magnitude*

The process of modelling minimum detectable magnitude at each grid point is described in *Section 3.3;* the initial results are shown in Figure 4.2.2. The initial model was built using only the stations that were active as of January 17, 2025; these stations are shown as black triangles. Included in Figure 4.2.2 are the missed ONC earthquakes, which were determined by comparing ONC data with NRCAN data; Appendix B provides a list of these events. An important note on these plotted missed ONC earthquakes, they are set up in QGIS such that the magnitude includes both the labelled magnitude itself and the magnitude 0.1 step below (i.e., magnitude 3.8 would also include magnitude 3.7).

Figure 4.2.2 shows the results of determining the minimum detectable earthquake magnitude at each grid point. For example, areas coloured blue represent a minimum magnitude of 3.0, meaning that at each of the grid points coloured blue, it is expected that any earthquake with a magnitude below 3.0 would not be detected, i.e., modelled ground motions do not reach the required threshold of 5 times the noise level at four stations. It is important to note that this model is limited by the GMPE, which is only accurate for magnitudes from 3.0-6.0; ground motions for magnitudes less than 3.0 were not calculated. Thus, in some of the areas coloured blue (M 3.0), it is likely that earthquakes of M < 3.0 would actually be detected; i.e., the minimum detectable magnitude is likely overestimated in the centre of the blue-coloured region.

The goal of creating this model was to understand if the missed earthquakes could be explained by the geometry of the stations. The missed earthquakes shown in Figure 4.2.2 are plotted with colours matching the magnitude threshold colours for easier analysis. If the missed earthquakes plotted only on "warmer" (higher) magnitude threshold colours (towards red) compared to their magnitude (e.g., a blue or green earthquake on a yellow or orange background), then we could conclude that the missed events can be explained purely by the geometry of the stations; however, this is not the case. For example, the missed magnitude 3.8 earthquake within the red box on Figure 4.2.2 plots in a "cooler" (lower) magnitude threshold area (3.0), where it "should" have been detected. This is one example of many missed earthquakes plotting on a minimum threshold level that is lower than the missed earthquake magnitude. None of the earthquakes plotted onto this map are explainable by station geometry, since they all plot onto lower magnitude ("cooler") threshold areas.

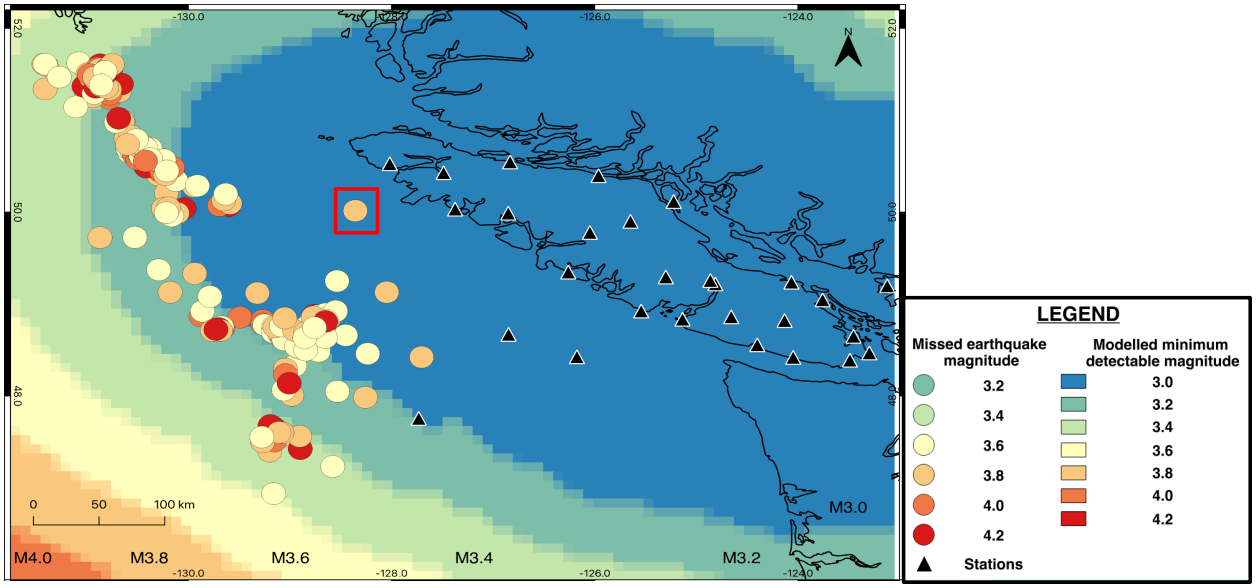


Figure 4.2.2. Minimum detectable earthquake magnitude modelled across the ONC grid, based on calculated ground motion exceeding 5 times the background noise at a minimum of 4 of the active stations (black triangles). Included on the map are the locations and magnitudes of earthquakes detected by NRCan, but missed by the ONC EEW system. The red box highlights an M3.8 event mentioned in the text. Coastline files were developed by Natural Earth https://www.naturalearthdata.com/downloads/10m-physical-vectors/10m-bathymetry/ tectonic boundaries were developed by USGS www.usgs.gov

## *4.3 Sensitivity Tests*

It seems unreasonable that none of the missed events can be explained by the geometry of the stations. Thus, in order to improve and understand the model further, sensitivity tests were conducted by changing the background noise level, the number of stations detecting sufficient signal, and the algorithm parameters.

### *4.3.1 Increasing Background Noise*

The first test was to increase the level of background noise, which previously was set at the average value determined for all stations (both on- and offshore). This noise level may have been significantly lower than actual values at many stations. First, the background noise level used in the model was increased to the highest background noise level for onshore stations, and then to the highest level for offshore stations using the information in Table 2. The highest background noise determined for onshore stations is 0.00003898 cm/s$^2$ from station CN_NTKA, and the highest offshore value is 0.0002459 cm/s$^2$ from NV_CBC27.

The result of this change in modelling is shown in Figure 4.3.1. The minimum magnitude threshold area has noticeably shrunk in radius, and now there is a new (higher) threshold area in the southwest corner for minimum magnitude 4.2. However, the M 3.8 event mentioned in *Section 4.2.2* and shown in the red box still plots within a region of lower magnitude threshold, as do other events. There are, however, some events that now fit significantly better (i.e., plotting on a cooler magnitude), such as the events within the blue box in the northwest corner (Figure 4.3.1).

The number of missed earthquakes that are explainable by the geometry of the stations is 5 whereas the number of unexplainable earthquakes is 226. For a total of 231 earthquakes, this makes the percent explainable earthquakes 2.0% (Figure 4.3.2; note these events are of magnitude 3.5 and hence are explainable since they lie within the 3.6 threshold) and unexplainable earthquakes 97.8% (Figure 4.3.3). This is a slight improvement from the 0% explainable earthquakes, based on modelling using a lower noise level.

The highest background noise is used in the remainder of modelling as this improves the accuracy of the model.

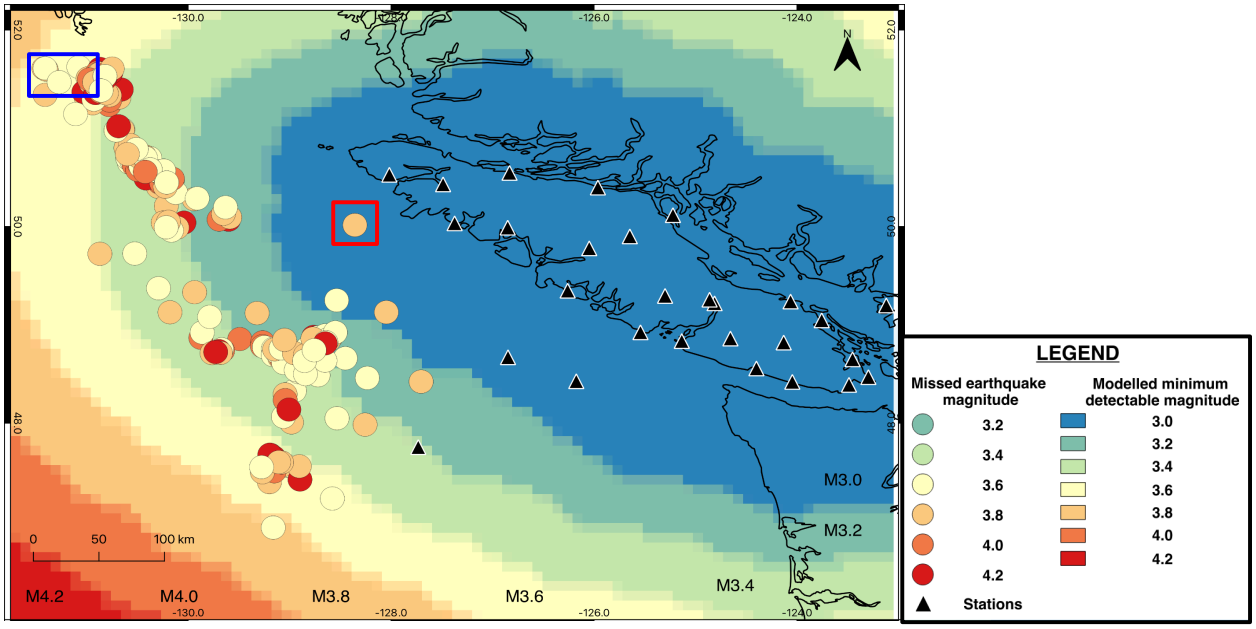


Figure 4.3.1. Results from modelling the minimum magnitude threshold of the ONC grid with the highest background noise. Included on the map are the missed ONC earthquakes. In the red box is the mentioned M3.8 event and in the blue box are other events mentioned in this section. Bathymetric and coastline files were developed by Natural Earth https://www.naturalearthdata.com/downloads/10m-physical-vectors/10m-bathymetry/ tectonic boundaries were developed by USGS www.usgs.gov

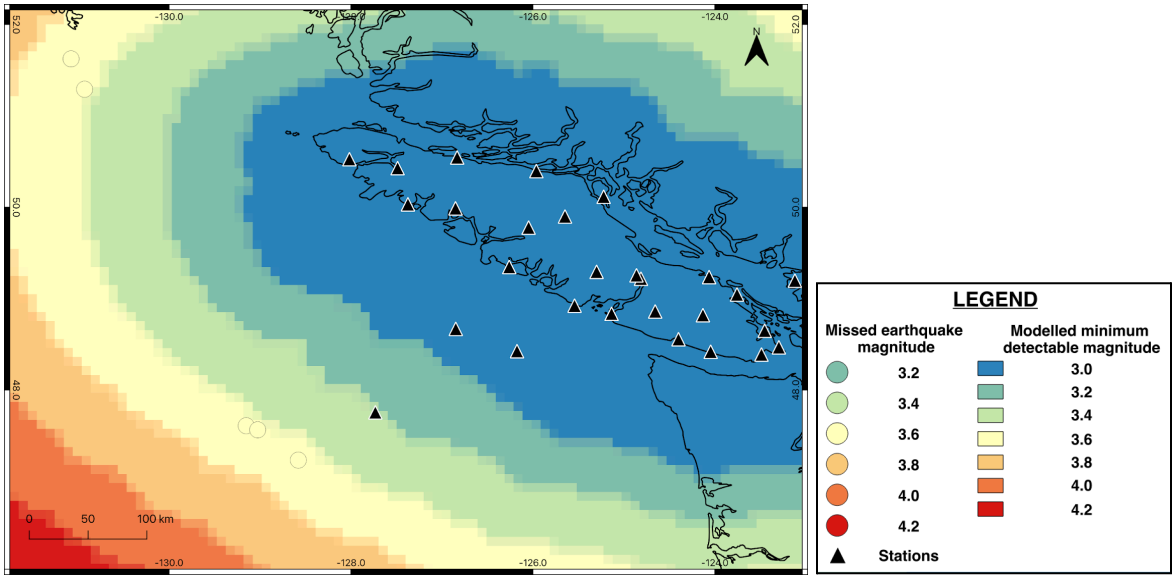


Figure 4.3.2. Map showing the missed earthquakes explainable by the geometry of the stations with highest background noise. Coastline files were developed by Natural Earth https://www.naturalearthdata.com/downloads/10m-physical-vectors/10m-bathymetry/ tectonic boundaries were developed by USGS www.usgs.gov

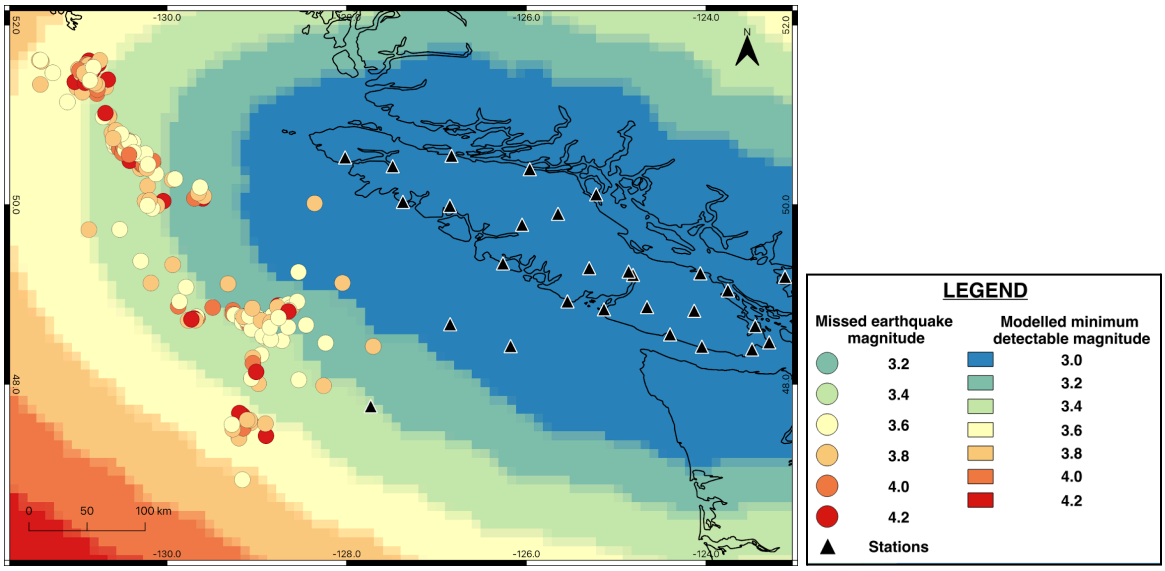


Figure 4.3.3. Map showing the missed earthquakes unexplainable by the geometry of the stations using a model with highest background noise. Coastline files were developed by Natural Earth https://www.naturalearthdata.com/downloads/10m-physical-vectors/10m-bathymetry/ tectonic boundaries were developed by USGS www.usgs.gov

*4.3.2 Adjusting Ground Motion Acceleration Values*

Increasing the background noise still resulted in a large and likely unreasonable number of unexplainable missed earthquakes. Another possible reason is that the modelling over-predicted the ground motion for given magnitudes. This is because GMPEs predict the strongest part of the waveform (maximum ground motion, i.e., S waves) as opposed to P waves, as analyzed in the EEW algorithms. Not taking this into account would result in an underprediction of the minimum detectable magnitude across the ONC grid, even when using a high level of background noise as shown in Figure 4.3.1. In order to compensate for the overprediction of ground motion, all predicted acceleration values were divided by a factor of 5, which is an approximate ratio of S wave to P wave values (Stein & Wysession, 2002). The result of incorporating this adjustment is shown in Figure 4.3.4.

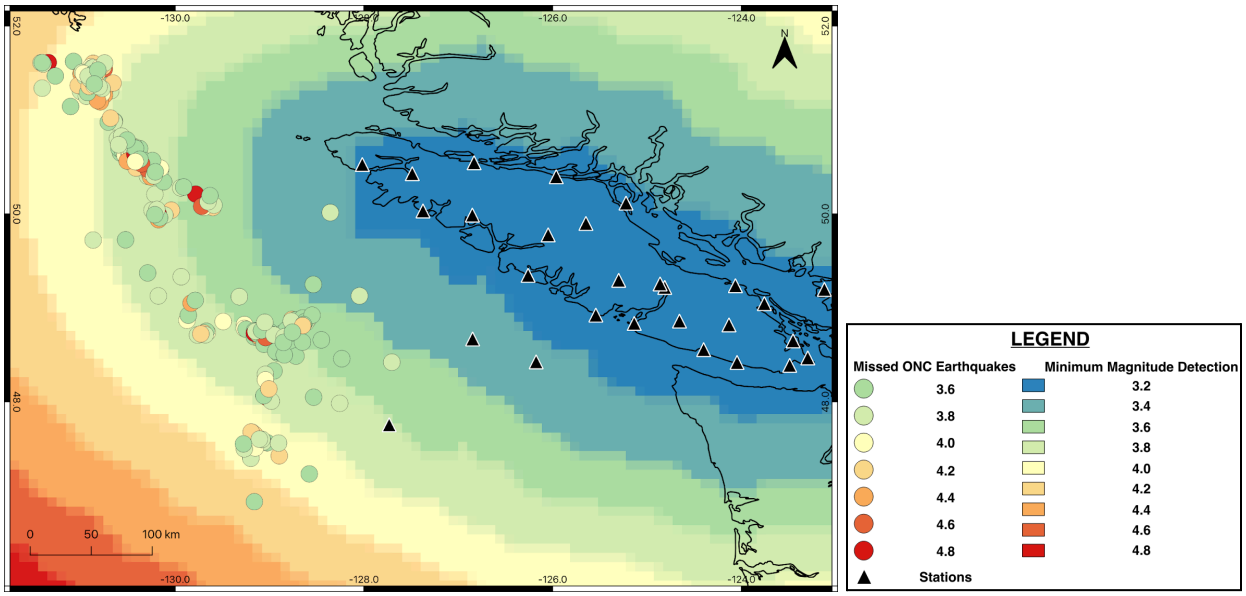


Figure 4.3.4. Results from dividing peak ground acceleration by 5 to compensate for overprediction as a result of GMPE predicting S wave rather than P wave amplitude; the highest background noise was used. Note that the blue coloured threshold has a higher detectable magnitude (3.2) compared to previous maps (3.0). Bathymetric and coastline files were developed by Natural Earth https://www.naturalearthdata.com/downloads/10m-physical-vectors/10m-bathymetry/ tectonic boundaries were developed by USGS www.usgs.gov

Also plotted on Figure 4.3.4 are the earthquakes missed by ONC. The number of missed earthquakes plotted is 264. With this new model, 129 or 48.9% of those are now explainable by the geometry of the stations (Figure 4.3.5), whereas 135 or 51.1% are unexplainable by the geometry of the stations (Figure 4.3.6). This is a significant change from the results of the initial modelling (Figure 4.3.1).

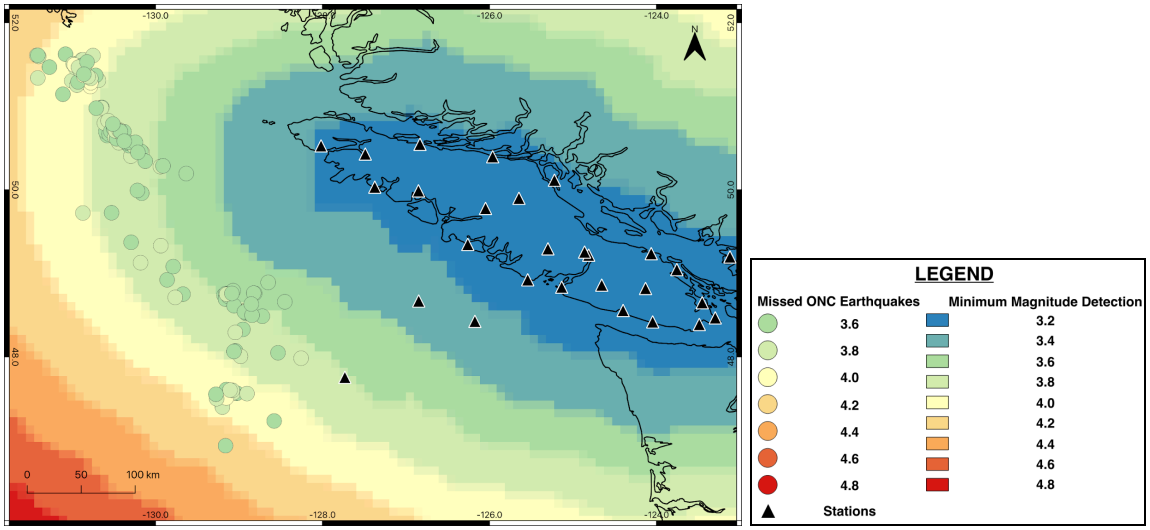


Figure 4.3.5. Map showing the missed earthquakes explainable by the geometry of the stations. Bathymetric and coastline files were developed by Natural Earth https://www.naturalearthdata.com/downloads/10m-physical-vectors/10m-bathymetry/ tectonic boundaries were developed by USGS www.usgs.gov

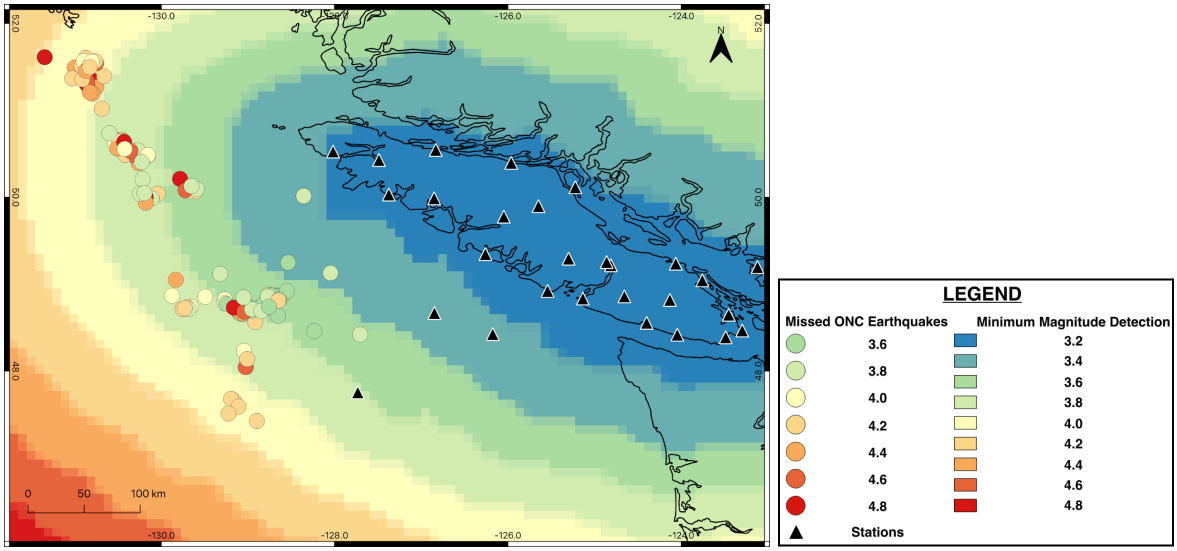


Figure 4.3.6 Map showing the missed earthquakes unexplainable by the geometry of the stations. Bathymetric and coastline files were developed by Natural Earth https://www.naturalearthdata.com/downloads/10m-physical-vectors/10m-bathymetry/ tectonic boundaries were developed by USGS www.usgs.gov

### *4.3.3 Changing Percentage of Active Stations Modelled*

One contributing factor as to whether enough stations will detect a sufficient P wave amplitude is how many stations are active on a given day. The station configuration scenario used to model the initial maps shown in Figures 4.2.2, 4.3.1, and 4.3.4 was from January 17, 2025. One sensitivity test conducted was to see how minimum detectable magnitude would change with different active station configurations; the list of all stations is provided in Table 4.

Tests were run with 30% and 50% of stations operating, with a random selection of which stations were active or inactive. For comparison, on January 17, 2025, ~45% of stations were operational.

Table 4. All ONC EEW stations that are accelerometers or accelerometers/GNSS

| Device Location | Latitude (°N) | Longitude (°W) |
|---|---|---|
| AL2H | 48.38981 | -123.48739 |
| BACME.W1 | 48.314627 | -126.05811 |
| BAMF | 48.83533 | -125.13514 |
| BCOV | 50.54427 | -126.84264 |
| BPEB | 50.15662 | -127.77188 |
| CBC27.W1 | 47.756685 | -127.73193 |
| CLRS | 48.82032 | -124.1309 |
| CMBR | 49.59497 | -125.01135 |
| CQS64.W1 | 48.699718 | -126.87262 |
| ELIZ | 49.87311 | -127.12162 |
| ERMD | 49.19781 | -123.11988 |
| FAHB | 50.060578 | -127.11469 |
| GLRI | 49.778594 | -126.04706 |
| HOLB | 50.64 | -128.135 |
| JRDR | 48.420143 | -124.04571 |
| KWOS | 50.23067 | -127.13392 |
| KYUQ | 50.03308 | -127.37367 |
| MGRB | 48.99973 | -124.69705 |
| MYRA | 49.5509 | -125.57053 |
| NANA | 49.237216 | -124.06302 |
| NC89.W1 | 48.670473 | -126.8477 |
| NCBC.W1 | 48.426575 | -126.17465 |
| NCSB | 50.40301 | -126.0559 |

| | | |
|---|---|---|
| NITI | 48.860686 | -124.65579 |
| NTKA | 49.5922 | -126.6168 |
| PALI | 50.429165 | -127.4873 |
| PGC5 | 48.64983 | -123.45206 |
| PHRD | 50.70615 | -127.51472 |
| PRAL.W1 | 49.218886 | -124.81181 |
| PREN | 48.556529 | -124.39959 |
| PTAL | 49.25632 | -124.8611 |
| PTRF | 48.54423 | -124.41304 |
| QISL | 50.11631 | -125.22219 |
| QUAD | 50.13247 | -125.33072 |
| SAYW | 50.397276 | -125.96176 |
| SC04 | 48.9233 | -123.70432 |
| SHPB | 49.3476 | -126.25979 |
| SNCH | 48.468465 | -123.29615 |
| STRA | 49.90003 | -125.64718 |
| SYMB | 48.55929 | -123.79893 |
| TAHB | 49.909675 | -126.66408 |
| TAYR | 49.294836 | -125.29989 |
| TELC | 50.545933 | -126.8324 |
| TFNO | 49.15434 | -125.90772 |
| UCLU | 48.92457 | -125.54198 |
| VICP | 50.00632 | -126.10854 |
| VIK.W1 | 50.03285 | -127.37447 |
| WINH | 50.52703 | -128.01686 |
| WOSB | 50.16078 | -126.57039 |
| YWPT | 49.046248 | -123.75631 |
| ZEBA.W3 | 49.98961 | -126.85058 |

The result of the 30% station operation is shown in Figure 4.3.7 and the result of the 50% station operation is shown in Figure 4.3.8. The minimum detectable magnitude threshold noticeably changes between the two different scenarios; for example, the M3.2 threshold area is much smaller in the 30% station scenario than the 50% scenario. The 50% scenario has approximately the same number of stations as the January 2025 active station configuration (Figure 4.3.4), but the contours have a different shape.

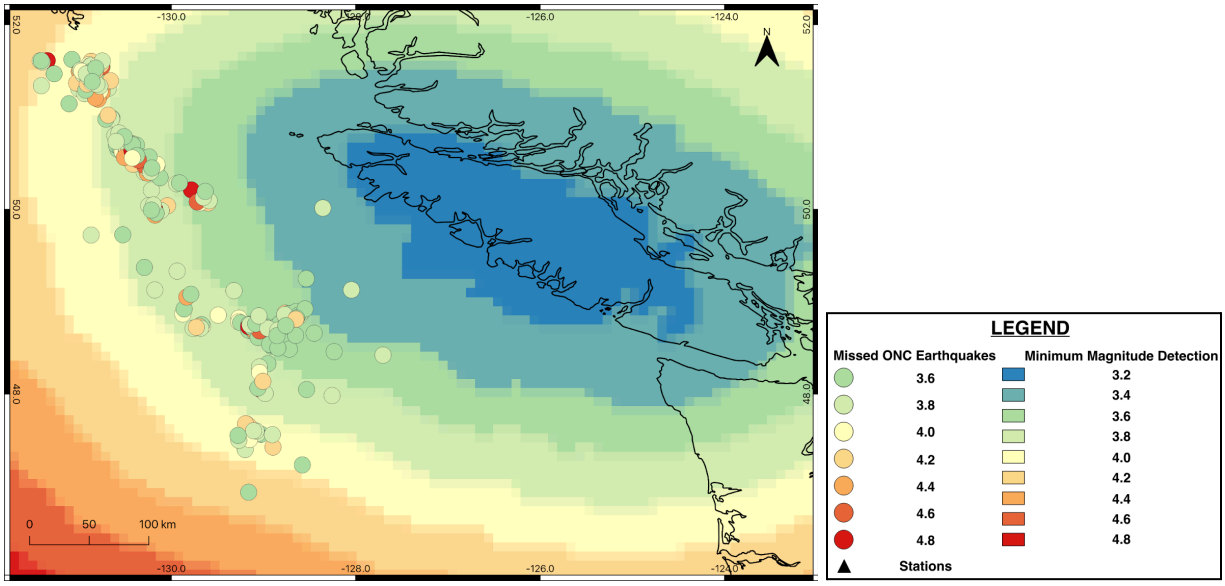


Figure 4.3.7. Results from modelling the ONC EEW grid with a random selection of 30% of active stations. Bathymetric and coastline files were developed by Natural Earth https://www.naturalearthdata.com/downloads/10m-physical-vectors/10m-bathymetry/ tectonic boundaries were developed by USGS www.usgs.gov

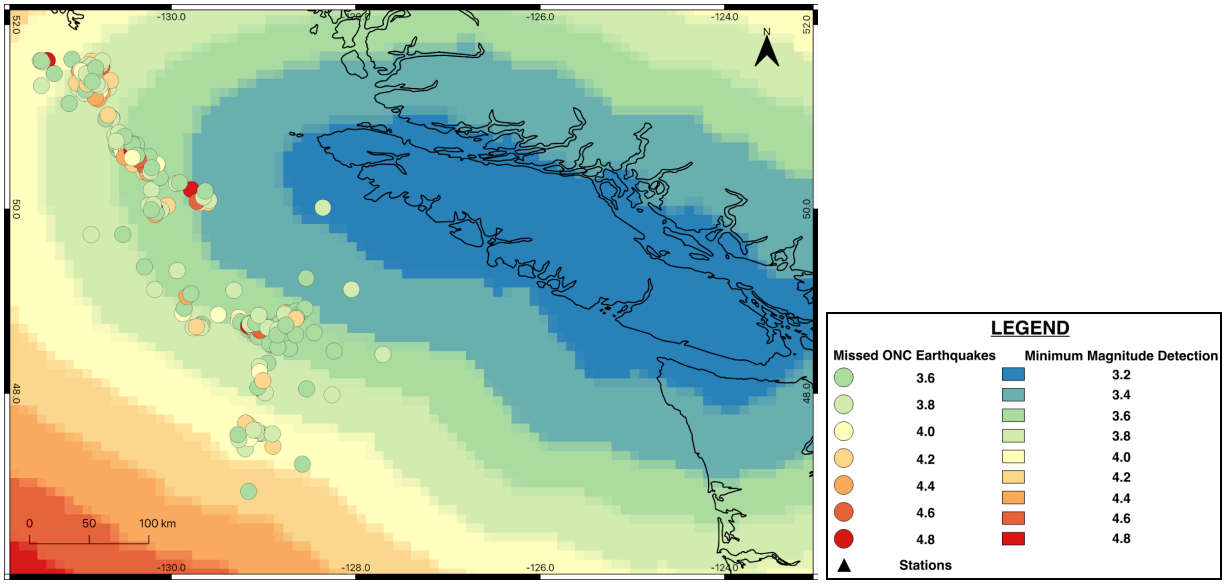


Figure 4.3.8. Results from modelling the ONC EEW grid with a random selection of 50% of active stations. Bathymetric and coastline files were developed by Natural Earth https://www.naturalearthdata.com/downloads/10m-physical-vectors/10m-bathymetry/ tectonic boundaries were developed by USGS www.usgs.gov

### *4.3.4 Decreasing System Algorithm Station Requirement To Three Stations*

In order to assess how the ONC EEW system could be optimized, a sensitivity test was run, to decrease the number of required stations for earthquake detection from four to three; the result is shown in Figure 4.3.9. This figure shows the result of modeling using 3 stations required for event detection, the highest background noise, and no adjusting of amplitude values (a) and the model shown in Figure 4.3.1 which uses a 4 station requirement, highest background noise, and no adjusting (b). Between these two models, there is a slight change in the threshold such that the 3.0 threshold in Figure 4.3.9(a) has a larger area than Figure 4.3.9(b). This indicates that decreasing the station requirement from 4 to 3 would increase event detection even slightly. There is not a super noticeable difference between this result and Figure 4.3.1.

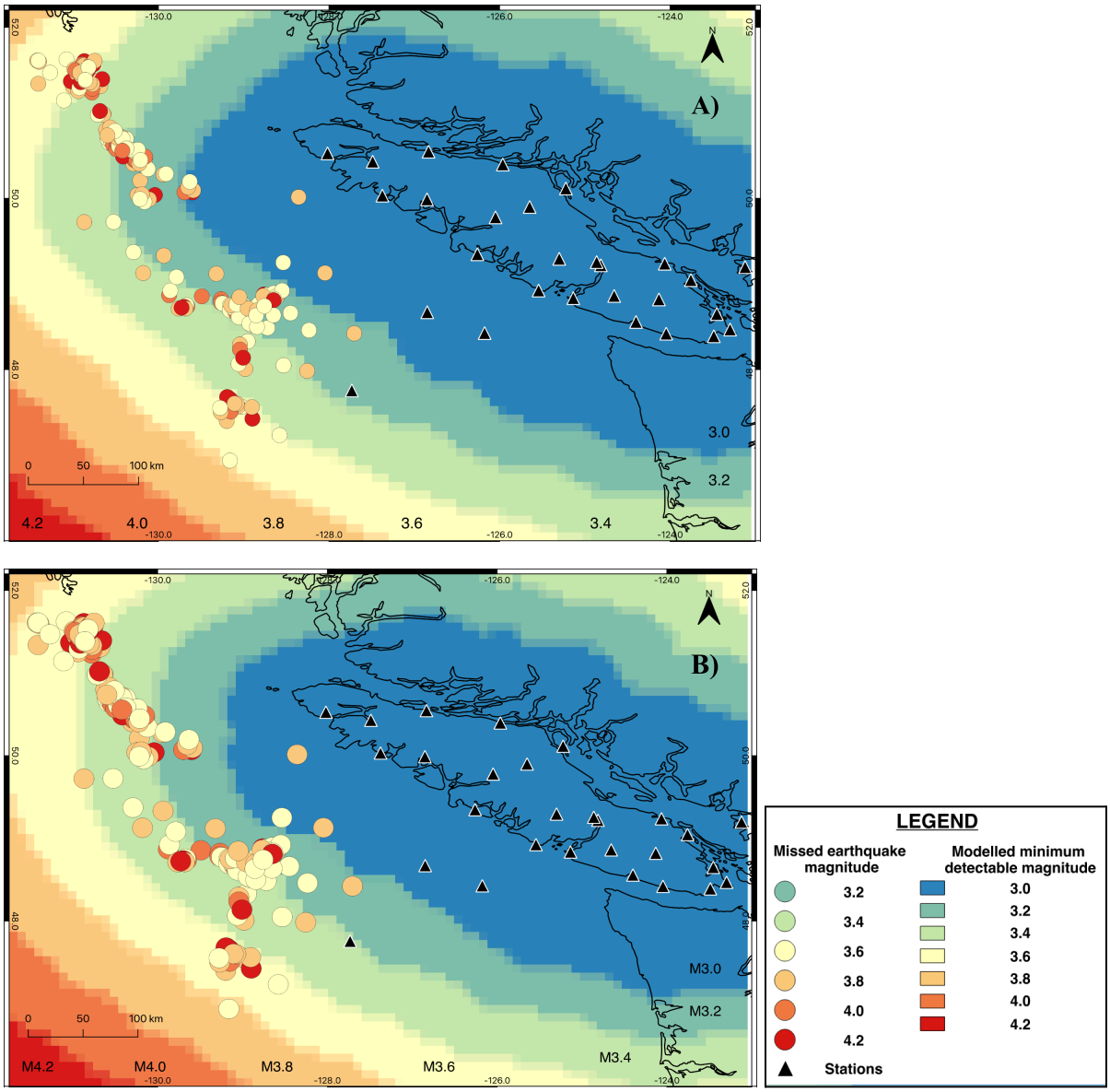


Figure 4.3.9. Results from decreasing number of required stations detecting P wave amplitude for earthquake associated from four stations (b) to three stations (a). Bathymetric and coastline files were developed by Natural Earth https://www.naturalearthdata.com/downloads/10m-physical-vectors/10m-bathymetry/ tectonic boundaries were developed by USGS www.usgs.gov

# 5.0 Discussion

## *5.1 Low Earthquake Detection Areas in the ONC EEW grid*

While the ONC EEW system has missed detection of earthquakes all along the boundary between the Pacific plate and the Juan de Fuca/Explorer plates (Figure 4.1d), two areas of the grid are missing proportionally the most earthquakes, as denoted by the red boxes in Figure 4.1.

The low-detection area in the northwest is of greater concern than the area in the southwest of the ONC grid. This is because the northwest portion of the ONC grid is an area which generates larger earthquakes than the southwest portion. The southwest portion of the grid is along the divergent plate boundary between the Juan de Fuca and Pacific plates (Figure 4.1). This area generally has shallower and lower magnitude seismicity, due to a shallow brittle-ductile transition in the region of the young and warm newly-formed oceanic plates, and thus is not a significant source of seismic hazard and risk to southwestern BC. The northwest region however is host to larger earthquakes (e.g., M 6.5 September 15, 2024 south of Haida Gwaii, see *Section 4.1.1*) and thus increasing the detection of earthquakes in the northwest area is a higher priority than the southwest.

## *5.2 Results of Modelling the Minimum Detectable Magnitude*

The final model using highest background noise and adjusting the amplitudes to better represent P waves, as shown in Figure 4.3.4, is the result of trying to understand why the ONC EEW system is missing earthquakes. The results show that 48.9% of the missed earthquakes are explainable by the geometry of the stations and 51.1% are unexplainable by the geometry. The question is, how accurate and representative are the modelled ground motions and earthquake detection to real events and conditions in the ONC EEW grid area? There are many parameters that could affect the accuracy of the model; it is impossible to develop a completely representative model. The following sub-sections will discuss the various uncertainties in the modelling.

### *5.2.1 Uncertainties in Ground Motion Prediction Equation*

In this study, P-wave amplitude was calculated using the GMPE of Atkinson (2005; Equations 3-5) and using offshore coefficients for all areas across the grid. As discussed in *Section 4.2.1,* the use of offshore coefficients creates a relatively low uncertainty at greater epicentre-station distances regardless of the magnitude values, but would cause an issue when the distances are shorter. Mostly, the four sets of curves (predicted ground motion for the four different earthquake location types) diverged from each other at distances of ~150 km (M6) to ~75 km (M3). Greatest uncertainties are expected for modelled ground motion in larger magnitude non-offshore earthquakes around Vancouver Island where most of the stations are

located. However, because the minimum detectable magnitudes are lowest in the Vancouver Island region, the uncertainty in detectability caused by just using the offshore coefficients is relatively low.

An additional source of uncertainty in the preliminary modelling was the calculation of P-wave amplitude using the GMPE. The GMPE predicts the maximum part of the waveform, which is generally the S wave. However, the ONC EEW network focuses on the largest P wave amplitude. S waves are typically 5 times larger than the P waves generated in the same earthquake. In an attempt to compensate for this, the modelled acceleration values were divided by 5. However, the factor of 5 is an approximation and the true ratio of the S- to P-wave amplitudes may vary, thus contributing uncertainty to the modelling. To more accurately predict P wave amplitudes, waveform simulations would provide more reliable results than the GMPE; such simulations are recommended for future work.

### *5.2.2 Uncertainties in Station Background Noise*

The station background noise level used in the final model (e.g., Figure 4.3.4) was the highest background noise of the onshore and offshore stations in Table 2. The data for background noise were recorded over different time periods across a range of stations. Seismic background noise can change at a station for various reasons, including variations in ocean wave noise from quiet sea states to significant storm activity. For this reason the seismic background noise at a station changes regularly and therefore there are uncertainties in using one seismic background study which only takes into account noise data over certain periods of time for only a handful of stations. Having a more comprehensive background noise study over all the stations over a larger period of time would make the assumed background noise more accurate and decrease the uncertainty in the modelling.

### *5.2.3 Uncertainties in Number of Active Stations*

There is also uncertainty in the number and locations of active ONC stations at a given time. As shown in *Section 4.3.3,* the number of active stations can have a significant impact on the minimum detectable earthquake magnitude across the grid. The 50% and 30% active stations scenarios illustrate that the magnitude thresholds for a given area can vary by up to ~0.2 magnitude units.

For the duration of modelling minimum detectable magnitude across the grid only the active stations on January 17, 2025 were used. As shown by changing the percentage of stations, the threshold can vary based on the configuration of active stations. Thus, just using one day to model magnitudes adds uncertainty to the accuracy of the model.

### *5.3 The Case Study: An Undetected M 6.5 Earthquake*

The M 6.5 event south of Haida Gwaii on September 15th, 2024 (Figure 4.1.1) likely went undetected by the ONC EEW system due to an error in epicentre determination. The event is considered invalid if the epicentre locations determined by 2 different methods differ by more than 80 km, which is likely what happened during this event. But why were the two epicentres so different that the event was considered invalid? Further investigation is warranted on this event to determine exactly. Investigating other missed events for similar patterns should also be carried out to determine if this is a common problem.

### *5.4 Are The Missed Earthquakes Explainable by the Geometry of the Stations?*

Can the results of modeling the minimum detectable magnitude across the ONC EEW grid determine if the missed events are explainable by the geometry of the stations? Even though Figure 4.3.4 shows that 48.9% of the stations are explainable by the geometry of the stations, it is hard to come to a definite conclusion because of the uncertainties in how accurately the model represents the real world scenario. However, as described in *Section 4.1.1,* investigation of the missed M 6.5 earthquake revealed that the event was determined to be invalid potentially because the two methods used by the algorithm to determine epicentre located the events more than 80 km apart. This discovery would suggest that the likely reason that the ONC earthquakes are going undetected is also explainable by the algorithm. Thus, the missed earthquakes are not only explainable by the geometry of the stations, but potentially by both geometry and other aspects of the algorithm.

### *5.5 Recommendations*

One of the goals of this research project was to provide information as to how the ONC EEW system could be optimized. For example, modelling could assess optimal locations for additional stations to improve the geometry of the network; however, placement of new stations

away from the existing cabled ONC infrastructure is not a realistic or achievable goal. Instead the main focus of recommendations resulting from this research centres around where the earthquake detection algorithm could be improved and what further research could be conducted.

The first recommendation is to conduct a full analysis of the missing ONC earthquakes, particularly in the northwestern area of the grid to determine the reasons for events going undetected (i.e., how many earthquakes are missed because there are not enough stations detecting P waves above their background noise) and how many are missed because there is another threshold not being met, even when enough stations detect sufficient P waves. This would narrow down the dominant reason for earthquakes going undetected by the ONC EEW system - the geometry of the stations versus other algorithm parameters. Analyses should cover not only the past missed earthquakes, but there should also be an analysis after each future missed event. Another recommendation is to carry out an analysis on the epicentre algorithm specifically, such as potentially increasing the 80 km requirement especially for events near the edges of the grid.

A final suggestion is that ONC consider the addition of more stations from the NRCAN Canadian National Seismograph Network (CNSN). Figure 5.5 shows the CNSN stations located on Haida Gwaii and the adjacent mainland coast. The addition of more stations would add coverage beyond the northwest area of the grid. This could decrease the minimum detectable earthquake magnitude across the grid both by increasing the number of stations that could detect sufficient P wave amplitudes, and enabling more accurate epicentral locations. Further to this, modelling could be conducted on how including stations from the Pacific Northwest Seismic Network would also increase earthquake detection accuracy.


Figure 5.5 Map of Haida Gwaii and coastal mainland BC. The blue dots are stations apart of the CNSN. Map is from https://www.earthquakescanada.nrcan.gc.ca/stndon/wf-fo/index-en.php

# 6.0 Conclusion

Ocean Networks Canada's Earthquake Early Warning system is an important addition to mitigative efforts against the impact of strong ground shaking of future large earthquakes in southwestern BC. Based on a comparison between the earthquake catalogs of ONC, NRCAN, and the USGS, the ONC system is noted to do a good job of detecting events around Vancouver Island and the Nootka fault zone, but further offshore the system has missed some events especially within the northwest and southwest areas of the grid (Figure 4.1). From January 2022 to February 2025 there were 271 missed events with a magnitude range of 3.5-6.5 within the ONC grid.

After modelling the minimum detectable earthquake magnitude across the ONC EEW grid, the results suggest that the system is missing a significant number of events because of the geometry of the stations (i.e., that too few stations are located within a range of detectable P waves, given that the system requires detection at a minimum of 4 stations). After adjusting the model to include a maximum value of background noise and adjusting the amplitudes modelled with ground motion prediction equations (GMPE, which effectively predict S wave amplitudes) to better represent lower-amplitude P wave values as detected by the EEW system, 48.9% of the earthquakes are explainable by the geometry of the stations. However, 51.1% of the undetected

earthquakes remain unexplained by the network geometry, i.e., the modelling suggests that these events should have been detected by at least 4 stations.

After investigating the undetected September 15, 2024 M 6.5 event, it was determined that the system is experiencing issues with its epicentre determination algorithm. One theory is that the two epicentre algorithms (DGS, LLS) are not meeting the requirement that the epicentres they calculate are within 80 km of each other. Not meeting this requirement would result in the event being considered invalid.

Thus, this thesis comes to the conclusion that the Ocean Networks Canada Earthquake Early warning system is likely missing events both because of the geometry of the stations as well as because of other aspects of the algorithm (i.e., epicentre determination). Further to this, a more detailed study should be completed on the 271 missed events, plus any new missed events post February 2025.

It is important to note that there are uncertainties in whether the model is accurate to real world conditions. For example, using an S- to P-wave ratio of 5 to adjust the modelled amplitude values is not an entirely accurate assumption. As well, active stations from only one day (January 17, 2025) were used throughout the duration of the modelling. Modelling using random selections of 30% and 50% of stations being active shows that the number and location of active stations on a given day changes the magnitude detection thresholds. Thus, using the active station configuration from only one point in time adds error and uncertainty. In order to come to a definite conclusion on the main cause of missed events, further modelling to address these uncertainties should be conducted (e.g., using a simulation of waveforms instead of GMPE, developing different models with varying active station configurations).

Based on this study, recommendations on how to improve the Earthquake Early Warning system include: incorporating stations from NRCAN on Haida Gwaii and improving the epicentre determination algorithm (e.g., increasing the 80 km requirement).

## References


Atkinson, G. M. (2005). Ground Motions for Earthquakes in Southwestern British Columbia and Northwestern Washington: Crustal, In-Slab, and Offshore Events. *Bulletin of the Seismological Society of America*, *95*(3), 1027–1044. https://doi.org/10.1785/0120040182

Atwater B., Nelson A., Clague J., Carver G., Yamaguchi D., Bobrowsky P., Bourgeois J., Darienzo M., Grant W., Hemphill-Haley E., Kelsey H., Jacoby G., Nishenko S., Palmer S., Peterson C., Reinhart M. (1995). Summary of Coastal Geologic Evidence for Past Great Earthquakes at the Cascadia Subduction Zone. Earthquake Spectra. 11. 1-18. 10.1193/1.1585800.

Babaie Mahani, A., Kao, H., Walker, D., Johnson, J., & Salas, C. (2016). Performance Evaluation of the Regional Seismograph Network in Northeast British Columbia, Canada, for Monitoring of Induced Seismicity. *Seismological Research Letters*, *87*(3), 648–660. https://doi.org/10.1785/0220150241

Babaie Mahani, A., Ferguson, E., & Pirenne, B. (2024). Magnitude Estimation and Site Characterization in Southwestern British Columbia: Application to Earthquake Early Warning. *Journal of Seismology*, *28*(3), 735–751. https://doi.org/10.1007/s10950-024-10216-5

Bostock, M. G., Christensen, N. I., & Peacock, S. M. (2019). Seismicity in Cascadia. *Lithos*, *332–333*, 55–66. https://doi.org/10.1016/j.lithos.2019.02.019

Cassidy, J., Rogers, G., Lamontagne, M., Halchuk, S., & Adams, J. (2010). Canada's Earthquakes: 'The Good, the Bad, and the Ugly.' *Geoscience Canada*, *37*(1), 1–16. Érudit.

Clague, J. J. (1997). Evidence for large earthquakes at the Cascadia Subduction Zone. *Reviews of Geophysics*, *35*(4), 439–460. https://doi.org/10.1029/97RG00222

Clague, J. J., Bobrowsky, P. T., & Hutchinson, I. (2000). A review of geological records of large tsunamis at Vancouver Island, British Columbia, and implications for hazard. *Quaternary Science Reviews*, *19*(9), 849–863. https://doi.org/10.1016/S0277-3791(99)00101-8

Cremen, G., & Galasso, C. (2020). Earthquake Early Warning: Recent Advances and Perspectives. *Earth-Science Reviews*, *205*, 103184. https://doi.org/10.1016/j.earscirev.2020.103184

Gillette M. D. & Silverman H. F. (2008). A Linear Closed-Form Algorithm for Source Localization From Time-Differences of Arrival. *IEEE Signal Processing Letters*, *15*, 1–4. https://doi.org/10.1109/LSP.2007.910324

Hersir, G. P., Guðnason, E. Á., & Flóvenz, Ó. G. (2022). 7.04—Geophysical Exploration Techniques. In T. M. Letcher (Ed.), *Comprehensive Renewable Energy (Second Edition)* (pp. 26–79). Elsevier. https://doi.org/10.1016/B978-0-12-819727-1.00128-X

Hoshiba, M. (2013). Real-time prediction of ground motion by Kirchhoff-Fresnel boundary integral equation method: Extended front detection method for Earthquake Early Warning. *Journal of Geophysical Research: Solid Earth*, *118*(3), 1038–1050. https://doi.org/10.1002/jgrb.50119

Hutchinson, J., Kao, H., Riedel, M., Obana, K., Wang, K., Kodaira, S., Takahashi, T., & Yamamoto, Y. (2023). Tectonic Evolution of the Nootka Fault Zone and Deformation of the Shallow Subducted Explorer plate in Northern Cascadia as Revealed by Earthquake Distributions and Seismic Tomography. *Scientific Reports*, *13*(1), 7873. https://doi.org/10.1038/s41598-023-33310-z

Leonard, L. J., Hyndman, R. D., & Mazzotti, S. (2004). Coseismic Subsidence in the 1700 Great Cascadia Earthquake: Coastal Estimates versus Elastic Dislocation Models. *GSA Bulletin*, *116*(5–6), 655–670. https://doi.org/10.1130/B25369.1

McGuire, J. J., Ulberg, C. W., Lux, A. I., Böse, M., Andrews, J. R., Smith, D. E., Crowell, B. W., Murray, J. R., Henson, I., Hartog, R., Felizardo, C., Huynh, M., Aranha, M., Parker, G. A., Baltay, A., Murray, M. H., Biasi, G. P., Guiwits, S., Saunders, J. K., Bunn, J. (2025). ShakeAlert® Version 3: Expected Performance in Large Earthquakes. *Bulletin of the Seismological Society of America*, *115*(2), 533–561. https://doi.org/10.1785/0120240189

Nakamura, Y., & Saita, J. (2007). UrEDAS, the Earthquake Warning System: Today and Tomorrow. In P. Gasparini, G. Manfredi, & J. Zschau (Eds.), *Earthquake Early Warning Systems* (pp. 249–281). Springer Berlin Heidelberg. https://doi.org/10.1007/978-3-540-72241-0_13

Schlesinger, A., Kukovica, J., Rosenberger, A., Heesemann, M., Pirenne, B., Robinson, J., & Morley, M. (2021). An Earthquake Early Warning System for Southwestern British Columbia. *Frontiers in Earth Science*, *9*. https://doi.org/10.3389/feart.2021.684084

Stein, S., & Wysession, M. (2002). *An Introduction to Seismology, Earthquakes, and Earth Structure*. Blackwell Publishing.

Suárez, G., Espinosa-Aranda, J. M., Cuéllar, A., Ibarrola, G., García, A., Zavala, M., Maldonado, S., & Islas, R. (2018). A Dedicated Seismic Early Warning Network: The Mexican Seismic Alert System (SASMEX). *Seismological Research Letters*, *89*(2A), 382–391. https://doi.org/10.1785/0220170184

# Appendix A

Table A1: ONC Earthquake Catalog including events from Jan 2022 to Feb 2025

| ID | Detailed Earthquake ID | Time | Organization | Magnitude | Latitude | Longitude |
|---|---|---|---|---|---|---|
| 13 | 13 | 2022-01-30T04:02:15.000Z | NRCAN | 3.6 | 48.0726 | -129.0415 |
| 12 | 12 | 2022-02-08T15:05:00.000Z | NRCAN | 3.5 | 50.6508 | -130.5788 |
| 11 | 11 | 2022-02-09T00:10:39.000Z | NRCAN | 3.6 | 48.4875 | -128.72 |
| 10 | 10 | 2022-02-12T08:33:39.000Z | NRCAN | 3.8 | 50.0158 | -128.3562 |
| 14 | 14 | 2022-02-22T14:25:59.000Z | NRCAN | 3.9 | 48.8558 | -129.491 |
| 15 | 740 | 2022-02-25T18:57:34.000Z | NRCAN | 3.3 | 49.7261 | -127.1318 |
| 16 | 17 | 2022-03-16T16:32:29.000Z | NRCAN | 3.8 | 50.4768 | -130.1544 |
| 17 | 741 | 2022-03-18T17:31:12.000Z | NRCAN | 2.2 | 49.5684 | -126.4952 |
| 18 | 20 | 2022-03-19T12:40:32.000Z | NRCAN | 3.8 | 49.1576 | -128.0249 |
| 20 | 22 | 2022-03-27T08:59:44.000Z | NRCAN | 3.7 | 51.3529 | -130.7868 |
| 19 | 21 | 2022-03-27T09:09:16.000Z | NRCAN | 3.7 | 51.2837 | -130.8967 |
| 21 | 24 | 2022-04-07T12:12:20.000Z | NRCAN | 3.9 | 48.9208 | -128.3113 |
| 22 | 29 | 2022-04-23T21:22:47.000Z | NRCAN | 5.3 | 50.195 | -129.7645 |
| 25 | 30 | 2022-05-01T23:19:04.000Z | NRCAN | 3.7 | 50.2791 | -129.941 |
| 115 | 179 | 2022-05-04T22:54:07.000Z | NRCAN | 3.5 | 48.553 | -128.9276 |
| 114 | 178 | 2022-05-05T03:38:11.000Z | NRCAN | 4.1 | 48.5661 | -128.9165 |
| 116 | 180 | 2022-05-11T06:11:34.000Z | NRCAN | 3.6 | 46.9375 | -129.1609 |
| 117 | 229 | 2022-05-18T07:12:55.000Z | NRCAN | 2.3 | 49.4792 | -127.039 |

| ID | Detailed Earthquake ID | Time | Organization | Magnitude | Latitude | Longitude |
|---|---|---|---|---|---|---|
| 118 | 182 | 2022-05-24T21:38:31.000Z | NRCAN | 3.7 | 50.4043 | -130.2942 |
| 119 | 183 | 2022-05-26T07:15:27.000Z | NRCAN | 3.5 | 47.6099 | -129.1517 |
| 120 | 184 | 2022-06-01T18:16:51.000Z | NRCAN | 3.7 | 51.6105 | -131.421 |
| 121 | 186 | 2022-06-04T23:59:10.000Z | NRCAN | 5.1 | 51.6219 | -131.4151 |
| 123 | 188 | 2022-06-13T17:34:39.000Z | NRCAN | 4.6 | 50.6509 | -130.5102 |
| 124 | 191 | 2022-06-19T00:36:45.000Z | NRCAN | 3.7 | 48.7233 | -129.0068 |
| 157 | 228 | 2022-07-12T11:43:33.000Z | NRCAN | 2.2 | 49.7728 | -127.7744 |
| 158 | 225 | 2022-07-14T16:32:12.000Z | NRCAN | 3.5 | 47.5652 | -129.0251 |
| 159 | 227 | 2022-07-19T02:14:48.000Z | NRCAN | 2.7 | 49.5743 | -127.119 |
| 161 | 232 | 2022-07-26T05:13:34.000Z | NRCAN | 3.7 | 51.5972 | -131.3987 |
| 160 | 231 | 2022-07-26T05:46:21.000Z | NRCAN | 4.8 | 51.6133 | -131.3443 |
| 162 | 233 | 2022-07-28T00:51:34.000Z | NRCAN | 3.6 | 51.611 | -131.409 |
| 164 | 237 | 2022-08-07T05:51:12.000Z | NRCAN | 3.6 | 50.9883 | -130.6432 |
| 163 | 236 | 2022-08-08T07:38:53.000Z | NRCAN | 4.7 | 48.7254 | -129.1079 |
| 165 | 238 | 2022-08-09T10:27:28.000Z | NRCAN | 3.6 | 48.7387 | -129.1791 |
| 166 | 239 | 2022-08-15T23:42:42.000Z | NRCAN | 3.6 | 49.7256 | -130.5257 |
| 167 | 241 | 2022-08-27T00:38:15.000Z | NRCAN | 3.5 | 49.4013 | -127.4674 |
| 168 | 742 | 2022-09-02T01:58:48.000Z | NRCAN | 2.2 | 49.7606 | -127.2605 |
| 169 | 243 | 2022-09-07T02:47:01.000Z | NRCAN | 3.6 | 50.6971 | -130.5951 |
| 171 | 247 | 2022-09-20T03:08:39.000Z | NRCAN | 4.1 | 49.3968 | -127.728 |

| ID | Detailed Earthquake ID | Time | Organization | Magnitude | Latitude | Longitude |
|---|---|---|---|---|---|---|
| 172 | 743 | 2022-09-20T08:36:46.000Z | NRCAN | 2.9 | 49.6573 | -127.4149 |
| 173 | 744 | 2022-09-22T14:41:57.000Z | NRCAN | 3.1 | 48.0882 | -124.675 |
| 174 | 249 | 2022-09-29T15:09:31.000Z | NRCAN | 3.8 | 47.5718 | -129.0669 |
| 175 | 250 | 2022-10-21T17:54:17.000Z | NRCAN | 3.8 | 50.5152 | -130.3024 |
| 176 | 251 | 2022-10-25T01:26:55.000Z | NRCAN | 3.8 | 51.3401 | -131.409 |
| 177 | 252 | 2022-10-31T03:18:40.000Z | NRCAN | 3.5 | 48.33 | -128.9525 |
| 334 | 433 | 2022-11-07T03:17:15.000Z | NRCAN | 4.2 | 50.3203 | -130.0449 |
| 335 | 434 | 2022-11-10T04:36:24.000Z | NRCAN | 3.5 | 51.6246 | -131.0772 |
| 336 | 435 | 2022-11-13T06:54:21.000Z | NRCAN | 3.7 | 50.9819 | -130.6462 |
| 337 | 438 | 2022-11-24T13:10:01.000Z | NRCAN | 4 | 47.6776 | -129.1875 |
| 338 | 446 | 2022-11-26T03:50:15.000Z | NRCAN | 4.8 | 49.2707 | -126.2493 |
| 339 | 441 | 2022-11-27T11:06:04.000Z | NRCAN | 3.5 | 50.6677 | -130.5554 |
| 340 | 442 | 2022-12-04T18:50:33.000Z | NRCAN | 3.9 | 50.4482 | -130.2823 |
| 342 | 445 | 2022-12-06T13:29:19.000Z | NRCAN | 5.2 | 50.5278 | -130.4713 |
| 343 | 447 | 2022-12-25T12:53:17.000Z | NRCAN | 3.9 | 48.8686 | -129.8747 |
| 345 | 449 | 2022-12-28T04:45:24.000Z | NRCAN | 4.1 | 47.6796 | -129.1949 |
| 344 | 448 | 2022-12-28T08:06:53.000Z | NRCAN | 4.2 | 47.6532 | -129.1574 |
| 346 | 450 | 2023-01-03T11:35:20.000Z | NRCAN | 3.5 | 48.9231 | -129.8607 |
| 574 | 746 | 2023-01-22T15:18:07.000Z | NRCAN | 3.7 | 49.7232 | -130.8693 |
| 578 | 751 | 2023-02-07T14:11:22.000Z | NRCAN | 3.8 | 48.8816 | -128.5886 |

| ID | Detailed Earthquake ID | Time | Organization | Magnitude | Latitude | Longitude |
|---|---|---|---|---|---|---|
| 577 | 750 | 2023-02-08T05:59:35.000Z | NRCAN | 4.2 | 50.0407 | -130.0408 |
| 579 | 752 | 2023-02-11T12:36:12.000Z | NRCAN | 3.7 | 51.3052 | -131.0023 |
| 582 | 756 | 2023-02-15T18:48:38.000Z | NRCAN | 3.7 | 50.8002 | -130.6122 |
| 580 | 753 | 2023-02-16T06:32:03.000Z | NRCAN | 3.9 | 48.8227 | -129.2656 |
| 581 | 754 | 2023-02-17T06:55:46.000Z | NRCAN | 4.8 | 50.2126 | -129.7826 |
| 586 | 760 | 2023-02-20T01:30:03.000Z | NRCAN | 3.9 | 50.4674 | -130.288 |
| 583 | 761 | 2023-02-20T09:08:36.000Z | NRCAN | 4.2 | 48.7466 | -129.1444 |
| 585 | 767 | 2023-02-20T10:31:55.000Z | NRCAN | 2.8 | 49.6568 | -127.0413 |
| 588 | 764 | 2023-02-20T11:02:50.000Z | NRCAN | 3.9 | 50.0978 | -129.6536 |
| 587 | 763 | 2023-02-21T03:12:59.000Z | NRCAN | 3.7 | 50.1016 | -129.6658 |
| 589 | 768 | 2023-03-06T02:24:33.000Z | NRCAN | 3.5 | 48.05 | -128.5325 |
| 591 | 771 | 2023-03-08T06:07:29.000Z | NRCAN | 4 | 50.0715 | -129.6946 |
| 590 | 770 | 2023-03-08T10:04:26.000Z | NRCAN | 4.1 | 50.07 | -129.6012 |
| 597 | 780 | 2023-03-08T15:24:50.000Z | NRCAN | 3.8 | 49.9895 | -130.1096 |
| 596 | 779 | 2023-03-08T16:47:51.000Z | NRCAN | 3.7 | 50.5644 | -130.4382 |
| 598 | 781 | 2023-03-09T19:29:10.000Z | NRCAN | 3.6 | 50.5295 | -130.3151 |
| 592 | 772 | 2023-03-12T15:31:54.000Z | NRCAN | 4.5 | 48.8137 | -129.6557 |
| 599 | 782 | 2023-03-15T09:00:16.000Z | NRCAN | 3.7 | 50.8288 | -130.5676 |
| 593 | 776 | 2023-03-19T14:45:26.000Z | NRCAN | 3.3 | 49.5815 | -127.3768 |
| 600 | 783 | 2023-03-24T23:09:13.000Z | NRCAN | 3.8 | 48.2936 | -129.0441 |

| ID | Detailed Earthquake ID | Time | Organization | Magnitude | Latitude | Longitude |
|---|---|---|---|---|---|---|
| 594 | 777 | 2023-03-30T15:01:45.000Z | NRCAN | 4 | 50.5366 | -130.2837 |
| 595 | 784 | 2023-04-02T01:08:31.000Z | NRCAN | 4.5 | 50.0813 | -129.7193 |
| 602 | 786 | 2023-04-03T01:51:42.000Z | NRCAN | 3.8 | 50.1303 | -129.652 |
| 601 | 785 | 2023-04-03T02:37:19.000Z | NRCAN | 3.7 | 50.095 | -129.5898 |
| 603 | 789 | 2023-04-13T15:54:54.000Z | NRCAN | 5.7 | 49.1051 | -129.6483 |
| 604 | 791 | 2023-04-13T16:05:11.000Z | NRCAN | 4.3 | 49.0511 | -129.8315 |
| 605 | 792 | 2023-04-13T22:45:37.000Z | NRCAN | 3.5 | 49.0815 | -129.7877 |
| 610 | 799 | 2023-04-14T13:22:22.000Z | NRCAN | 3.6 | 48.7736 | -129.2484 |
| 606 | 800 | 2023-04-14T15:49:05.000Z | NRCAN | 4 | 48.7829 | -129.2676 |
| 609 | 798 | 2023-04-14T19:06:00.000Z | NRCAN | 4.1 | 47.5907 | -129.1071 |
| 607 | 796 | 2023-04-19T18:56:28.000Z | NRCAN | 4.5 | 48.8892 | -129.3059 |
| 611 | 801 | 2023-05-01T00:55:19.000Z | NRCAN | 3.7 | 51.2846 | -130.7964 |
| 613 | 803 | 2023-05-02T05:41:44.000Z | NRCAN | 3.6 | 50.5622 | -130.3422 |
| 612 | 802 | 2023-05-02T08:51:08.000Z | NRCAN | 3.7 | 50.5776 | -130.3619 |
| 615 | 805 | 2023-05-27T21:56:00.000Z | NRCAN | 3.7 | 49.1282 | -130.1786 |
| 614 | 804 | 2023-06-01T15:03:04.000Z | NRCAN | 3.7 | 50.5203 | -130.255 |
| 616 | 806 | 2023-06-03T12:55:54.000Z | NRCAN | 3.7 | 47.9848 | -128.2561 |
| 617 | 807 | 2023-06-11T21:39:25.000Z | NRCAN | 4 | 50.463 | -130.2613 |
| 618 | 808 | 2023-06-18T00:17:54.000Z | NRCAN | 4.1 | 50.4896 | -130.4148 |
| 619 | 809 | 2023-06-20T04:12:44.000Z | NRCAN | 4.3 | 50.3943 | -130.2594 |

| ID | Detailed Earthquake ID | Time | Organization | Magnitude | Latitude | Longitude |
|---|---|---|---|---|---|---|
| 620 | 810 | 2023-06-20T04:28:27.000Z | NRCAN | 3.7 | 50.4504 | -130.1601 |
| 621 | 811 | 2023-06-20T07:40:35.000Z | NRCAN | 3.6 | 50.4622 | -130.1747 |
| 622 | 813 | 2023-06-22T23:37:31.000Z | NRCAN | 3.9 | 50.4416 | -130.2614 |
| 623 | 814 | 2023-07-05T06:19:52.000Z | NRCAN | 3.8 | 50.2094 | -130.215 |
| 624 | 817 | 2023-07-07T09:12:34.000Z | NRCAN | 2.5 | 48.3372 | -123.0094 |
| 625 | 819 | 2023-07-27T05:31:58.000Z | NRCAN | 3.7 | 50.7151 | -130.5214 |
| 627 | 821 | 2023-07-29T09:12:33.000Z | NRCAN | 3.6 | 50.7023 | -130.5351 |
| 629 | 823 | 2023-08-30T00:57:31.000Z | NRCAN | 3.6 | 50.7357 | -130.5014 |
| 630 | 825 | 2023-09-04T11:37:35.000Z | NRCAN | 3.3 | 51.1103 | -125.2005 |
| 638 | 833 | 2023-09-14T17:03:37.000Z | NRCAN | 3.7 | 50.6817 | -130.4249 |
| 637 | 832 | 2023-09-14T17:12:22.000Z | NRCAN | 3.7 | 50.6303 | -130.4872 |
| 636 | 831 | 2023-09-14T17:15:42.000Z | NRCAN | 4 | 50.6608 | -130.4568 |
| 635 | 830 | 2023-09-14T17:27:10.000Z | NRCAN | 3.9 | 50.6256 | -130.5323 |
| 634 | 829 | 2023-09-14T17:31:06.000Z | NRCAN | 4.2 | 50.6583 | -130.4471 |
| 633 | 828 | 2023-09-14T17:41:29.000Z | NRCAN | 4.3 | 50.6413 | -130.4797 |
| 632 | 827 | 2023-09-14T17:52:26.000Z | NRCAN | 4.1 | 50.6614 | -130.5134 |
| 631 | 826 | 2023-09-14T18:02:47.000Z | NRCAN | 4 | 50.6497 | -130.4835 |
| 644 | 842 | 2023-09-15T03:35:38.000Z | NRCAN | 4 | 50.6392 | -130.4832 |
| 643 | 841 | 2023-09-17T09:42:44.000Z | NRCAN | 4 | 50.577 | -130.4968 |
| 641 | 838 | 2023-09-17T09:58:57.000Z | NRCAN | 4.5 | 50.609 | -130.4833 |

| ID | Detailed Earthquake ID | Time | Organization | Magnitude | Latitude | Longitude |
|---|---|---|---|---|---|---|
| 639 | 837 | 2023-09-17T11:28:08.000Z | NRCAN | 5.4 | 50.6079 | -130.533 |
| 642 | 839 | 2023-09-17T15:19:49.000Z | NRCAN | 4.4 | 50.652 | -130.4561 |
| 646 | 844 | 2023-09-17T15:58:34.000Z | NRCAN | 3.7 | 50.693 | -130.436 |
| 645 | 843 | 2023-09-17T19:23:58.000Z | NRCAN | 3.5 | 50.6121 | -130.4655 |
| 649 | 848 | 2023-09-19T11:47:47.000Z | NRCAN | 3.7 | 50.7074 | -130.48 |
| 647 | 846 | 2023-09-25T13:31:47.000Z | NRCAN | 4.1 | 47.4262 | -128.8975 |
| 648 | 847 | 2023-09-26T02:09:09.000Z | NRCAN | 4.1 | 47.511 | -129.2241 |
| 650 | 850 | 2023-09-28T12:33:30.000Z | NRCAN | 2.5 | 49.4629 | -126.7768 |
| 651 | 851 | 2023-10-07T22:17:31.000Z | NRCAN | 3.6 | 50.6974 | -130.3777 |
| 697 | 915 | 2023-10-09T02:21:08.000Z | NRCAN | 4 | 48.0385 | -122.7547 |
| 654 | 856 | 2023-10-10T06:19:58.000Z | NRCAN | 3.5 | 48.6603 | -128.4509 |
| 653 | 853 | 2023-10-11T07:15:54.000Z | NRCAN | 3.9 | 51.2373 | -130.78 |
| 652 | 852 | 2023-10-11T11:15:24.000Z | NRCAN | 4.3 | 50.5636 | -130.5084 |
| 655 | 857 | 2023-10-16T03:13:52.000Z | NRCAN | 4.9 | 50.5334 | -130.3604 |
| 656 | 859 | 2023-10-24T05:58:20.000Z | NRCAN | 4.6 | 50.4749 | -130.2889 |
| 661 | 866 | 2023-11-21T16:22:11.000Z | NRCAN | 3.5 | 50.3439 | -130.122 |
| 660 | 865 | 2023-11-21T17:11:03.000Z | NRCAN | 3.8 | 49.12 | -129.3202 |
| 659 | 864 | 2023-11-23T05:18:31.000Z | NRCAN | 3.7 | 47.3998 | -129.1986 |
| 662 | 867 | 2023-11-26T15:32:17.000Z | NRCAN | 3.6 | 48.7568 | -129.1592 |
| 663 | 870 | 2023-11-30T02:53:07.000Z | NRCAN | 2.4 | 49.2963 | -125.2773 |

| ID | Detailed Earthquake ID | Time | Organization | Magnitude | Latitude | Longitude |
|---|---|---|---|---|---|---|
| 664 | 871 | 2023-12-17T23:23:15.000Z | NRCAN | 4.7 | 51.1629 | -124.4493 |
| 666 | 875 | 2024-01-02T00:06:29.000Z | NRCAN | 3.8 | 50.5408 | -130.2707 |
| 667 | 876 | 2024-01-03T03:54:18.000Z | NRCAN | 3.9 | 50.4875 | -130.1551 |
| 669 | 878 | 2024-01-07T12:00:13.000Z | NRCAN | 3.6 | 50.5693 | -130.3243 |
| 668 | 877 | 2024-01-07T18:11:44.000Z | NRCAN | 3.5 | 48.7929 | -129.0699 |
| 670 | 879 | 2024-01-09T01:41:26.000Z | NRCAN | 4.8 | 50.6373 | -130.4279 |
| 671 | 881 | 2024-01-09T03:52:05.000Z | NRCAN | 3.5 | 50.1956 | -129.6316 |
| 672 | 882 | 2024-01-09T15:15:43.000Z | NRCAN | 3.7 | 50.7157 | -130.4299 |
| 674 | 885 | 2024-01-16T22:24:01.000Z | NRCAN | 2.9 | 48.2277 | -124.8653 |
| 675 | 887 | 2024-01-22T00:48:43.000Z | NRCAN | 3.6 | 50.5696 | -130.2401 |
| 676 | 889 | 2024-01-26T17:11:07.000Z | NRCAN | 3.2 | 49.8383 | -123.5823 |
| 677 | 891 | 2024-01-30T06:23:18.000Z | NRCAN | 4.5 | 50.5343 | -130.3549 |
| 678 | 892 | 2024-02-01T07:44:19.000Z | NRCAN | 3.7 | 51.2541 | -130.9406 |
| 679 | 893 | 2024-02-01T11:23:43.000Z | NRCAN | 3.8 | 48.4227 | -127.7039 |
| 682 | 897 | 2024-02-01T21:14:01.000Z | NRCAN | 3.6 | 50.7001 | -130.4204 |
| 681 | 896 | 2024-02-03T02:02:35.000Z | NRCAN | 3.7 | 50.7081 | -130.4342 |
| 684 | 900 | 2024-02-04T10:44:11.000Z | NRCAN | 3.7 | 47.6006 | -129.079 |
| 683 | 899 | 2024-02-04T11:02:52.000Z | NRCAN | 3.7 | 47.5615 | -128.904 |
| 685 | 901 | 2024-02-04T14:10:24.000Z | NRCAN | 3.8 | 47.5003 | -129.2674 |
| 680 | 898 | 2024-02-05T07:33:13.000Z | NRCAN | 3.9 | 47.5098 | -129.1513 |

| ID | Detailed Earthquake ID | Time | Organization | Magnitude | Latitude | Longitude |
|---|---|---|---|---|---|---|
| 686 | 902 | 2024-02-06T01:34:20.000Z | NRCAN | 3.7 | 47.6035 | -129.1073 |
| 687 | 903 | 2024-02-10T07:31:02.000Z | NRCAN | 3.5 | 47.2335 | -128.5787 |
| 688 | 904 | 2024-02-11T19:56:03.000Z | NRCAN | 3.6 | 51.4697 | -131.2703 |
| 691 | 907 | 2024-02-18T22:01:41.000Z | NRCAN | 3.6 | 50.5832 | -130.3739 |
| 690 | 906 | 2024-02-18T23:18:14.000Z | NRCAN | 3.6 | 51.145 | -131.1085 |
| 692 | 909 | 2024-02-24T05:53:42.000Z | NRCAN | 3.9 | 49.3275 | -128.2331 |
| 696 | 914 | 2024-03-06T07:13:25.000Z | NRCAN | 3.6 | 48.0662 | -129.0604 |
| 695 | 913 | 2024-03-06T07:15:48.000Z | NRCAN | 3.7 | 48.0078 | -128.9815 |
| 693 | 910 | 2024-03-06T08:41:27.000Z | NRCAN | 4.6 | 48.0459 | -129.0248 |
| 694 | 912 | 2024-03-06T09:02:39.000Z | NRCAN | 3.7 | 49.3324 | -129.9361 |
| 699 | 918 | 2024-03-08T10:59:52.000Z | NRCAN | 3.6 | 48.4601 | -128.2342 |
| 698 | 917 | 2024-03-09T13:25:30.000Z | NRCAN | 3.7 | 49.1288 | -128.0463 |
| 700 | 919 | 2024-03-10T04:36:57.000Z | NRCAN | 3.9 | 48.7388 | -129.6597 |
| 701 | 920 | 2024-03-10T05:01:40.000Z | NRCAN | 3.9 | 48.725 | -129.6995 |
| 702 | 921 | 2024-03-10T07:49:06.000Z | NRCAN | 3.6 | 48.752 | -129.6702 |
| 703 | 922 | 2024-03-10T09:33:41.000Z | NRCAN | 4.2 | 48.7335 | -129.6976 |
| 710 | 929 | 2024-03-10T09:35:24.000Z | NRCAN | 4.2 | 48.7238 | -129.7282 |
| 704 | 923 | 2024-03-10T09:41:17.000Z | NRCAN | 4.2 | 48.7146 | -129.7546 |
| 705 | 924 | 2024-03-10T09:53:53.000Z | NRCAN | 3.6 | 48.6924 | -129.1615 |
| 709 | 928 | 2024-03-10T10:13:04.000Z | NRCAN | 3.8 | 48.7148 | -129.6812 |

| ID | Detailed Earthquake ID | Time | Organization | Magnitude | Latitude | Longitude |
|---|---|---|---|---|---|---|
| 707 | 926 | 2024-03-10T12:18:31.000Z | NRCAN | 3.8 | 48.7127 | -129.7639 |
| 706 | 925 | 2024-03-10T13:14:40.000Z | NRCAN | 3.8 | 48.6692 | -129.0972 |
| 708 | 927 | 2024-03-10T13:28:49.000Z | NRCAN | 3.9 | 48.6625 | -129.082 |
| 718 | 937 | 2024-03-11T11:50:42.000Z | NRCAN | 3.7 | 48.7087 | -129.044 |
| 716 | 935 | 2024-03-11T13:28:37.000Z | NRCAN | 3.6 | 48.7457 | -128.9947 |
| 711 | 930 | 2024-03-12T01:22:25.000Z | NRCAN | 3.6 | 48.6796 | -129.0377 |
| 714 | 933 | 2024-03-12T02:33:00.000Z | NRCAN | 3.8 | 48.7391 | -129.0082 |
| 713 | 932 | 2024-03-12T06:39:52.000Z | NRCAN | 3.6 | 48.6574 | -129.0592 |
| 715 | 934 | 2024-03-12T11:19:18.000Z | NRCAN | 3.6 | 48.6982 | -128.9491 |
| 721 | 942 | 2024-03-12T11:48:14.000Z | NRCAN | 3.6 | 48.7205 | -128.9805 |
| 712 | 931 | 2024-03-12T17:05:41.000Z | NRCAN | 3.7 | 48.8324 | -128.6497 |
| 717 | 940 | 2024-03-21T07:04:44.000Z | NRCAN | 2.3 | 48.6009 | -124.8109 |
| 719 | 943 | 2024-03-22T08:57:14.000Z | NRCAN | 2.5 | 49.7063 | -127.1377 |
| 720 | 941 | 2024-03-26T19:48:47.000Z | NRCAN | 3.6 | 50.7882 | -130.5103 |
| 722 | 945 | 2024-04-01T00:17:25.000Z | NRCAN | 3.4 | 49.6735 | -126.7521 |
| 725 | 949 | 2024-04-17T21:46:13.000Z | NRCAN | 4.9 | 49.9959 | -130.0883 |
| 726 | 951 | 2024-04-18T06:06:01.000Z | NRCAN | 4.8 | 50.0007 | -130.1785 |
| 731 | 959 | 2024-04-18T06:23:51.000Z | NRCAN | 3.6 | 49.9929 | -130.216 |
| 727 | 953 | 2024-04-18T06:41:42.000Z | NRCAN | 4.4 | 49.9391 | -130.1767 |
| 729 | 955 | 2024-04-18T07:36:37.000Z | NRCAN | 3.5 | 49.96 | -130.1644 |

| ID | Detailed Earthquake ID | Time | Organization | Magnitude | Latitude | Longitude |
|---|---|---|---|---|---|---|
| 730 | 958 | 2024-04-18T08:40:09.000Z | NRCAN | 3.8 | 50.0487 | -130.1936 |
| 728 | 954 | 2024-04-18T09:18:23.000Z | NRCAN | 3.8 | 50.0405 | -130.2452 |
| 733 | 961 | 2024-04-27T22:17:17.000Z | NRCAN | 3.6 | 49.3726 | -130.2915 |
| 732 | 960 | 2024-04-28T20:58:52.000Z | NRCAN | 3.6 | 48.732 | -128.8639 |
| 734 | 962 | 2024-05-03T03:03:28.000Z | NRCAN | 4.8 | 48.7613 | -128.8393 |
| 738 | 968 | 2024-05-03T03:06:21.000Z | NRCAN | 3.6 | 48.7273 | -128.7774 |
| 735 | 965 | 2024-05-03T03:13:51.000Z | NRCAN | 3.5 | 48.7614 | -128.8122 |
| 737 | 967 | 2024-05-03T05:04:32.000Z | NRCAN | 3.5 | 48.7643 | -128.8239 |
| 736 | 966 | 2024-05-03T05:50:24.000Z | NRCAN | 3.6 | 48.7672 | -128.82 |
| 739 | 970 | 2024-05-10T11:44:38.000Z | NRCAN | 4.3 | 48.7427 | -128.8287 |
| 740 | 972 | 2024-05-17T06:38:26.000Z | NRCAN | 3.6 | 47.5531 | -129.2761 |
| 741 | 973 | 2024-06-28T17:54:32.000Z | NRCAN | 3.9 | 50.5574 | -130.4222 |
| 742 | 974 | 2024-07-01T19:18:18.000Z | NRCAN | 3.8 | 50.7378 | -130.5986 |
| 743 | 975 | 2024-07-03T19:59:12.000Z | NRCAN | 3.9 | 48.2346 | -129.0432 |
| 744 | 977 | 2024-07-03T20:12:45.000Z | NRCAN | 4.1 | 48.1386 | -129.007 |
| 800 | 1065 | 2024-07-04T02:22:47.000Z | NRCAN | 3.5 | 48.4997 | -128.8438 |
| 749 | 996 | 2024-07-04T05:01:22.000Z | NRCAN | 3.6 | 48.5198 | -128.9124 |
| 757 | 998 | 2024-07-04T12:31:35.000Z | NRCAN | 3.6 | 48.6135 | -129.0588 |
| 750 | 983 | 2024-07-04T13:18:03.000Z | NRCAN | 4.9 | 48.6917 | -129.2656 |
| 753 | 992 | 2024-07-04T16:00:19.000Z | NRCAN | 4.4 | 48.6645 | -129.0635 |

| ID | Detailed Earthquake ID | Time | Organization | Magnitude | Latitude | Longitude |
|---|---|---|---|---|---|---|
| 751 | 985 | 2024-07-04T16:15:08.000Z | NRCAN | 5.7 | 48.6421 | -129.0613 |
| 754 | 990 | 2024-07-04T17:43:18.000Z | NRCAN | 4.4 | 48.6987 | -129.1115 |
| 755 | 994 | 2024-07-04T18:31:25.000Z | NRCAN | 4.7 | 48.7307 | -129.1616 |
| 756 | 997 | 2024-07-04T18:43:24.000Z | NRCAN | 3.6 | 48.724 | -129.1254 |
| 767 | 1012 | 2024-07-04T19:10:14.000Z | NRCAN | 3.5 | 48.5394 | -128.9343 |
| 765 | 1010 | 2024-07-04T20:44:00.000Z | NRCAN | 3.7 | 48.7508 | -129.1477 |
| 758 | 1007 | 2024-07-04T21:20:19.000Z | NRCAN | 3.7 | 48.5625 | -128.9081 |
| 764 | 1009 | 2024-07-04T23:13:29.000Z | NRCAN | 3.7 | 48.5228 | -128.8717 |
| 766 | 1011 | 2024-07-05T01:48:43.000Z | NRCAN | 3.6 | 48.5212 | -128.8768 |
| 763 | 1008 | 2024-07-05T02:09:00.000Z | NRCAN | 4.5 | 48.6843 | -129.0421 |
| 761 | 1003 | 2024-07-05T15:51:51.000Z | NRCAN | 3.9 | 48.6302 | -128.9982 |
| 762 | 1004 | 2024-07-05T16:34:05.000Z | NRCAN | 5.3 | 48.6186 | -128.9898 |
| 772 | 1023 | 2024-07-05T18:50:34.000Z | NRCAN | 3.5 | 48.7612 | -129.0847 |
| 768 | 1013 | 2024-07-06T11:01:06.000Z | NRCAN | 4.1 | 48.3224 | -129.0371 |
| 770 | 1018 | 2024-07-08T15:06:44.000Z | NRCAN | 5.2 | 48.647 | -129.0347 |
| 771 | 1021 | 2024-07-08T17:05:53.000Z | NRCAN | 4.4 | 48.6039 | -128.9395 |
| 774 | 1026 | 2024-07-11T15:08:32.000Z | NRCAN | 3.3 | 48.7068 | -128.8242 |
| 802 | 1067 | 2024-07-11T15:17:35.000Z | NRCAN | 4.1 | 48.8119 | -128.649 |
| 773 | 1025 | 2024-07-11T15:35:43.000Z | NRCAN | 4 | 48.8532 | -128.6748 |
| 801 | 1066 | 2024-07-11T15:58:56.000Z | NRCAN | 3.6 | 48.8244 | -128.6421 |

| ID | Detailed Earthquake ID | Time | Organization | Magnitude | Latitude | Longitude |
|---|---|---|---|---|---|---|
| 775 | 1029 | 2024-07-11T16:17:20.000Z | NRCAN | 5.2 | 48.8306 | -128.6096 |
| 781 | 1042 | 2024-07-11T16:44:34.000Z | NRCAN | 3.8 | 48.7128 | -128.9533 |
| 783 | 1044 | 2024-07-11T17:24:59.000Z | NRCAN | 3.7 | 48.6924 | -128.8444 |
| 776 | 1032 | 2024-07-11T17:34:26.000Z | NRCAN | 4.6 | 48.7983 | -128.6927 |
| 778 | 1037 | 2024-07-11T17:41:27.000Z | NRCAN | 3.7 | 48.8449 | -128.6138 |
| 777 | 1036 | 2024-07-11T17:48:30.000Z | NRCAN | 3.6 | 48.6363 | -128.6512 |
| 782 | 1043 | 2024-07-11T20:31:28.000Z | NRCAN | 3.6 | 48.871 | -128.7205 |
| 798 | 1063 | 2024-07-12T04:33:55.000Z | NRCAN | 3.8 | 48.8605 | -128.7701 |
| 779 | 1038 | 2024-07-12T08:20:28.000Z | NRCAN | 4.6 | 48.8581 | -128.7252 |
| 788 | 1051 | 2024-07-12T19:37:37.000Z | NRCAN | 3.6 | 48.8676 | -128.6669 |
| 791 | 1054 | 2024-07-12T20:00:08.000Z | NRCAN | 3.8 | 48.8627 | -128.6954 |
| 787 | 1050 | 2024-07-12T23:36:39.000Z | NRCAN | 3.7 | 48.856 | -128.6652 |
| 794 | 1057 | 2024-07-13T11:05:15.000Z | NRCAN | 3.6 | 48.8716 | -128.7289 |
| 797 | 1060 | 2024-07-13T11:15:50.000Z | NRCAN | 3.8 | 50.4058 | -130.2253 |
| 785 | 1048 | 2024-07-14T02:25:18.000Z | NRCAN | 4.1 | 48.8778 | -128.7634 |
| 799 | 1064 | 2024-07-14T06:37:13.000Z | NRCAN | 3.6 | 48.923 | -128.5495 |
| 793 | 1056 | 2024-07-15T03:54:24.000Z | NRCAN | 3.7 | 48.862 | -128.745 |
| 796 | 1059 | 2024-07-15T16:13:36.000Z | NRCAN | 3.6 | 48.8526 | -128.625 |
| 792 | 1101 | 2024-07-15T21:09:40.000Z | NRCAN | 2.6 | 49.8279 | -123.5772 |
| 795 | 1058 | 2024-07-16T01:44:39.000Z | NRCAN | 3.5 | 48.8924 | -128.6503 |

| ID | Detailed Earthquake ID | Time | Organization | Magnitude | Latitude | Longitude |
|---|---|---|---|---|---|---|
| 803 | 1070 | 2024-07-23T16:12:11.000Z | NRCAN | 4.6 | 50.4263 | -130.2512 |
| 804 | 1074 | 2024-07-24T18:41:43.000Z | NRCAN | 3.5 | 50.449 | -130.2106 |
| 805 | 1078 | 2024-08-02T08:19:26.000Z | NRCAN | 4 | 48.6645 | -128.7304 |
| 806 | 1104 | 2024-08-07T04:49:01.000Z | NRCAN | 2.4 | 48.7905 | -125.4888 |
| 807 | 1081 | 2024-08-09T06:14:15.000Z | NRCAN | 3.6 | 50.6885 | -124.4825 |
| 808 | 1106 | 2024-08-14T00:08:06.000Z | NRCAN | 3.5 | 48.8586 | -128.3365 |
| 809 | 1084 | 2024-08-23T10:23:35.000Z | NRCAN | 3.7 | 48.7314 | -128.7842 |
| 810 | 1103 | 2024-08-26T15:15:35.000Z | NRCAN | 2.8 | 48.8229 | -126.0263 |
| 811 | 1086 | 2024-09-04T15:32:26.000Z | NRCAN | 3.6 | 48.6334 | -128.8528 |
| 812 | 1087 | 2024-09-07T22:30:03.000Z | NRCAN | 3.5 | 50.9784 | -130.71 |
| 817 | 1093 | 2024-09-15T21:39:51.000Z | NRCAN | 4.5 | 51.5439 | -130.7515 |
| 841 | 1125 | 2024-09-15T22:01:46.000Z | NRCAN | 4 | 51.5076 | -130.8382 |
| 813 | 1088 | 2024-09-15T22:22:43.000Z | NRCAN | 6.5 | 51.3643 | -130.9513 |
| 821 | 1097 | 2024-09-15T22:34:32.000Z | NRCAN | 4.3 | 51.5731 | -130.8485 |
| 829 | 1111 | 2024-09-15T22:41:41.000Z | NRCAN | 4.1 | 51.3691 | -131.027 |
| 858 | 1145 | 2024-09-15T22:46:56.000Z | NRCAN | 3.8 | 51.558 | -130.8688 |
| 830 | 1113 | 2024-09-15T22:47:56.000Z | NRCAN | 4.1 | 51.3941 | -130.6585 |
| 861 | 1148 | 2024-09-15T22:50:13.000Z | NRCAN | 3.9 | 51.4969 | -130.973 |
| 849 | 1133 | 2024-09-15T23:01:01.000Z | NRCAN | 4.1 | 51.3585 | -130.9116 |
| 820 | 1096 | 2024-09-15T23:03:47.000Z | NRCAN | 4.3 | 51.4944 | -130.9977 |

| ID | Detailed Earthquake ID | Time | Organization | Magnitude | Latitude | Longitude |
|---|---|---|---|---|---|---|
| 814 | 1090 | 2024-09-15T23:26:45.000Z | NRCAN | 4.5 | 51.3648 | -130.8723 |
| 837 | 1121 | 2024-09-15T23:44:39.000Z | NRCAN | 4.3 | 51.2081 | -130.8228 |
| 851 | 1135 | 2024-09-15T23:52:20.000Z | NRCAN | 4 | 51.3712 | -130.8606 |
| 860 | 1147 | 2024-09-15T23:59:58.000Z | NRCAN | 3.7 | 51.608 | -130.748 |
| 823 | 1099 | 2024-09-16T00:32:09.000Z | NRCAN | 3.8 | 51.3122 | -130.682 |
| 840 | 1124 | 2024-09-16T00:33:19.000Z | NRCAN | 4 | 51.5679 | -130.8931 |
| 827 | 1109 | 2024-09-16T00:46:22.000Z | NRCAN | 4.1 | 51.6045 | -130.869 |
| 825 | 1107 | 2024-09-16T00:54:55.000Z | NRCAN | 4.4 | 51.2668 | -130.7499 |
| 819 | 1095 | 2024-09-16T01:27:36.000Z | NRCAN | 4.6 | 51.2731 | -130.8374 |
| 816 | 1116 | 2024-09-16T01:43:25.000Z | NRCAN | 4.8 | 51.359 | -130.8154 |
| 846 | 1130 | 2024-09-16T01:48:39.000Z | NRCAN | 3.6 | 51.4076 | -130.8755 |
| 853 | 1137 | 2024-09-16T02:09:16.000Z | NRCAN | 3.8 | 51.3554 | -130.8059 |
| 836 | 1120 | 2024-09-16T02:53:02.000Z | NRCAN | 4 | 51.5225 | -130.8261 |
| 832 | 1115 | 2024-09-16T03:30:30.000Z | NRCAN | 4.5 | 51.3304 | -130.8548 |
| 852 | 1136 | 2024-09-16T04:32:12.000Z | NRCAN | 3.8 | 51.5559 | -130.88 |
| 859 | 1146 | 2024-09-16T04:37:15.000Z | NRCAN | 4 | 51.5602 | -130.7991 |
| 848 | 1132 | 2024-09-16T04:39:21.000Z | NRCAN | 3.5 | 51.2923 | -130.9281 |
| 824 | 1100 | 2024-09-16T11:43:12.000Z | NRCAN | 3.6 | 51.3701 | -130.7152 |
| 843 | 1127 | 2024-09-16T11:48:29.000Z | NRCAN | 4 | 51.4719 | -130.8959 |
| 839 | 1123 | 2024-09-16T11:53:16.000Z | NRCAN | 4.2 | 51.5669 | -130.7614 |

| ID | Detailed Earthquake ID | Time | Organization | Magnitude | Latitude | Longitude |
|---|---|---|---|---|---|---|
| 822 | 1098 | 2024-09-16T12:50:20.000Z | NRCAN | 3.8 | 51.5092 | -130.9854 |
| 818 | 1094 | 2024-09-16T16:08:01.000Z | NRCAN | 4.5 | 51.2583 | -130.7789 |
| 845 | 1129 | 2024-09-16T19:01:03.000Z | NRCAN | 3.8 | 51.3352 | -130.7748 |
| 831 | 1114 | 2024-09-16T19:48:47.000Z | NRCAN | 3.6 | 51.538 | -130.8427 |
| 842 | 1126 | 2024-09-17T04:00:35.000Z | NRCAN | 4 | 51.3769 | -130.8555 |
| 833 | 1117 | 2024-09-17T08:12:24.000Z | NRCAN | 4.3 | 51.1945 | -130.7934 |
| 826 | 1108 | 2024-09-17T14:08:44.000Z | NRCAN | 4.2 | 51.511 | -130.918 |
| 834 | 1118 | 2024-09-18T01:31:02.000Z | NRCAN | 3.7 | 51.4621 | -130.9567 |
| 828 | 1112 | 2024-09-18T12:02:09.000Z | NRCAN | 4.7 | 51.3016 | -130.8575 |
| 838 | 1122 | 2024-09-19T09:58:58.000Z | NRCAN | 4.2 | 51.0211 | -130.6851 |
| 835 | 1119 | 2024-09-20T02:22:56.000Z | NRCAN | 3.9 | 51.2822 | -130.7744 |
| 844 | 1128 | 2024-09-22T07:02:58.000Z | NRCAN | 3.6 | 51.5406 | -130.8757 |
| 847 | 1131 | 2024-09-23T23:02:20.000Z | NRCAN | 3.6 | 51.5123 | -130.9311 |
| 850 | 1138 | 2024-09-25T01:33:23.000Z | NRCAN | 2.7 | 50.0566 | -127.9624 |
| 855 | 1142 | 2024-09-25T23:48:29.000Z | NRCAN | 3.7 | 51.4602 | -130.8828 |
| 856 | 1143 | 2024-09-26T06:24:16.000Z | NRCAN | 3.8 | 51.441 | -130.9079 |
| 854 | 1141 | 2024-09-26T11:05:19.000Z | NRCAN | 3.8 | 48.574 | -123.2843 |
| 857 | 1144 | 2024-09-26T12:08:15.000Z | NRCAN | 4.3 | 51.4548 | -130.8698 |
| 862 | 1149 | 2024-09-28T06:12:07.000Z | NRCAN | 3.6 | 51.4935 | -130.8722 |
| 863 | 1152 | 2024-10-02T15:35:46.000Z | NRCAN | 4.2 | 48.8564 | -129.5261 |

| ID | Detailed Earthquake ID | Time | Organization | Magnitude | Latitude | Longitude |
|---|---|---|---|---|---|---|
| 864 | 1154 | 2024-10-02T20:25:54.000Z | NRCAN | 2.6 | 49.6844 | -126.7516 |
| 865 | 1155 | 2024-10-04T09:08:57.000Z | NRCAN | 3.6 | 49.0402 | -123.3671 |
| 866 | 1159 | 2024-10-04T21:58:09.000Z | NRCAN | 4.1 | 51.4983 | -130.8246 |
| 868 | 1161 | 2024-10-05T13:55:50.000Z | NRCAN | 3.7 | 51.4687 | -130.9216 |
| 867 | 1160 | 2024-10-05T17:51:45.000Z | NRCAN | 3.7 | 51.4784 | -130.853 |
| 870 | 1165 | 2024-10-08T09:04:52.000Z | NRCAN | 3.6 | 50.2875 | -129.9101 |
| 869 | 1164 | 2024-10-08T13:59:36.000Z | NRCAN | 4 | 51.2991 | -126.0486 |
| 872 | 1168 | 2024-10-09T07:11:18.000Z | NRCAN | 3.6 | 51.5315 | -130.8195 |
| 871 | 1167 | 2024-10-10T06:50:59.000Z | NRCAN | 3.6 | 49.2505 | -128.5362 |
| 874 | 1170 | 2024-10-12T08:35:07.000Z | NRCAN | 3.6 | 51.3847 | -130.8574 |
| 873 | 1169 | 2024-10-15T13:05:17.000Z | NRCAN | 3.7 | 48.8472 | -129.0502 |
| 875 | 1171 | 2024-10-21T02:05:47.000Z | NRCAN | 3.6 | 48.7423 | -128.7578 |
| 876 | 1172 | 2024-10-24T18:44:08.000Z | NRCAN | 4 | 51.447 | -130.9049 |
| 878 | 1174 | 2024-10-28T03:11:43.000Z | NRCAN | 4.1 | 48.773 | -129.1672 |
| 877 | 1173 | 2024-10-28T13:24:27.000Z | NRCAN | 4 | 50.8643 | -130.7821 |
| 879 | 1175 | 2024-10-29T04:06:34.000Z | NRCAN | 3.7 | 48.736 | -129.1701 |
| 880 | 1176 | 2024-10-29T15:11:04.000Z | NRCAN | 3.5 | 48.7695 | -129.2339 |
| 881 | 1177 | 2024-11-05T18:57:07.000Z | NRCAN | 4.3 | 51.4637 | -130.9239 |
| 882 | 1178 | 2024-11-06T23:08:47.000Z | NRCAN | 4.2 | 51.5402 | -130.7773 |
| 885 | 1181 | 2024-11-09T12:07:38.000Z | NRCAN | 3.6 | 48.81 | -129.3204 |

| ID | Detailed Earthquake ID | Time | Organization | Magnitude | Latitude | Longitude |
|---|---|---|---|---|---|---|
| 884 | 1180 | 2024-11-10T02:50:21.000Z | NRCAN | 3.5 | 48.8216 | -129.3507 |
| 883 | 1179 | 2024-11-11T00:34:11.000Z | NRCAN | 3.5 | 50.5454 | -130.3245 |
| 886 | 1182 | 2024-11-13T19:30:01.000Z | NRCAN | 3.6 | 51.5228 | -130.7903 |
| 887 | 1183 | 2024-11-18T03:31:01.000Z | NRCAN | 3.7 | 50.6189 | -130.3531 |
| 888 | 1184 | 2024-11-21T12:14:16.000Z | NRCAN | 3.6 | 49.4155 | -128.1672 |
| 890 | 1187 | 2024-11-27T04:36:26.000Z | NRCAN | 3.6 | 51.2651 | -131.2092 |
| 893 | 1190 | 2024-11-30T13:18:02.000Z | NRCAN | 4 | 50.5096 | -130.2224 |
| 891 | 1188 | 2024-12-01T22:13:50.000Z | NRCAN | 3.7 | 46.4078 | -129.4272 |
| 892 | 1189 | 2024-12-03T14:51:48.000Z | NRCAN | 3.5 | 49.3986 | -130.2602 |
| 894 | 1192 | 2024-12-06T06:31:58.000Z | NRCAN | 4.5 | 48.9372 | -129.4807 |
| 899 | 1199 | 2024-12-09T07:01:34.000Z | NRCAN | 3.7 | 48.8589 | -129.4259 |
| 895 | 1194 | 2024-12-09T22:21:17.000Z | NRCAN | 3.6 | 51.4584 | -131.0041 |
| 897 | 1196 | 2024-12-13T00:17:58.000Z | NRCAN | 3.8 | 50.8571 | -130.5397 |
| 896 | 1198 | 2024-12-13T04:32:33.000Z | NRCAN | 3.3 | 49.6903 | -127.0981 |
| 902 | 1203 | 2024-12-22T11:02:46.000Z | NRCAN | 3.5 | 51.9062 | -130.9196 |
| 900 | 1201 | 2024-12-25T21:39:28.000Z | NRCAN | 4.8 | 50.5673 | -130.4223 |
| 901 | 1202 | 2025-01-06T22:07:50.000Z | NRCAN | 3.8 | 50.7369 | -130.4964 |
| 904 | 1205 | 2025-01-10T23:22:00.000Z | NRCAN | 3.7 | 48.7251 | -128.8827 |
| 903 | 1204 | 2025-01-12T07:16:13.000Z | NRCAN | 3.5 | 51.3574 | -130.7701 |
| 905 | 1206 | 2025-01-16T11:50:56.000Z | NRCAN | 3.7 | 51.4509 | -130.8177 |

| ID | Detailed Earthquake ID | Time | Organization | Magnitude | Latitude | Longitude |
|---|---|---|---|---|---|---|
| 908 | 1209 | 2025-01-29T16:02:46.000Z | NRCAN | 3.7 | 51.4563 | -130.9282 |
| 909 | 1211 | 2025-01-30T12:48:26.000Z | NRCAN | 3.7 | 51.968 | -126.2029 |
| 910 | 1212 | 2025-02-03T00:25:34.000Z | NRCAN | 4.3 | 51.3496 | -131.1535 |
| 911 | 1214 | 2025-02-06T12:05:46.000Z | NRCAN | 4.6 | 50.3782 | -130.1827 |
| 912 | 1217 | 2025-02-14T05:59:18.000Z | NRCAN | 3.6 | 48.2975 | -123.291 |
| 914 | 1220 | 2025-02-15T19:53:48.000Z | NRCAN | 3.7 | 48.6024 | -128.8879 |
| 915 | 1221 | 2025-02-16T09:46:39.000Z | NRCAN | 3.7 | 51.571 | -130.983 |
| 916 | 1222 | 2025-02-16T19:06:48.000Z | NRCAN | 3.7 | 49.4473 | -128.4594 |
| 913 | 1219 | 2025-02-17T16:54:02.000Z | NRCAN | 4 | 48.7713 | -129.2045 |
| 15 | 15 | 2022-02-25T18:57:36.819Z | Ocean Networks Canada Society | 2.6 | 49.89 | -127.02 |
| 17 | 18 | 2022-03-18T17:31:14.402Z | Ocean Networks Canada Society | 2.7 | 49.56 | -126.52 |
| 18 | 19 | 2022-03-19T12:40:31.005Z | Ocean Networks Canada Society | 3.9 | 49.02 | -128.08 |
| 21 | 23 | 2022-04-07T12:12:21.415Z | Ocean Networks Canada Society | 3.3 | 48.8 | -128.27 |
| 24 | 28 | 2022-04-23T21:22:39.857Z | Ocean Networks Canada Society | 4.9 | 50.18 | -130.88 |
| 22 | 25 | 2022-04-23T21:22:52.350Z | Ocean Networks Canada Society | 4.6 | 50.19 | -129.29 |
| 23 | 27 | 2022-04-23T21:23:30.662Z | Ocean Networks Canada Society | 4 | 49.56 | -125.75 |
| 117 | 181 | 2022-05-18T07:12:48.043Z | Ocean Networks Canada Society | 3.5 | 49.18 | -127.53 |
| 122 | 187 | 2022-06-13T17:35:05.839Z | Ocean Networks Canada Society | 3.6 | 50.3 | -127.69 |
| 157 | 224 | 2022-07-12T11:43:32.739Z | Ocean Networks Canada Society | 3.4 | 49.66 | -127.9 |
| 159 | 226 | 2022-07-19T02:14:46.734Z | Ocean Networks Canada Society | 3.2 | 49.54 | -127.18 |

| ID | Detailed Earthquake ID | Time | Organization | Magnitude | Latitude | Longitude |
|---|---|---|---|---|---|---|
| 163 | 234 | 2022-08-08T07:39:01.716Z | Ocean Networks Canada Society | 3.8 | 48.86 | -128.62 |
| 167 | 240 | 2022-08-27T00:38:18.916Z | Ocean Networks Canada Society | 3.2 | 49.64 | -127.42 |
| 168 | 242 | 2022-09-02T01:58:48.854Z | Ocean Networks Canada Society | 3.4 | 49.81 | -127.24 |
| 171 | 245 | 2022-09-20T03:08:42.286Z | Ocean Networks Canada Society | 3.6 | 49.36 | -127.78 |
| 170 | 244 | 2022-09-20T08:36:35.113Z | Ocean Networks Canada Society | 3.6 | 48.89 | -128.02 |
| 172 | 246 | 2022-09-20T08:36:44.703Z | Ocean Networks Canada Society | 3.2 | 49.64 | -127.44 |
| 173 | 248 | 2022-09-22T14:42:01.698Z | Ocean Networks Canada Society | 3.3 | 48.25 | -124.72 |
| 334 | 432 | 2022-11-07T03:17:18.854Z | Ocean Networks Canada Society | 3.9 | 50.27 | -129.66 |
| 338 | 439 | 2022-11-26T03:50:17.459Z | Ocean Networks Canada Society | 4.7 | 49.27 | -126.23 |
| 341 | 443 | 2022-12-06T13:29:30.903Z | Ocean Networks Canada Society | 4 | 50.5 | -129.34 |
| 583 | 757 | 2023-02-20T09:08:39.392Z | Ocean Networks Canada Society | 3.5 | 48.78 | -128.92 |
| 585 | 759 | 2023-02-20T10:31:55.894Z | Ocean Networks Canada Society | 3.2 | 49.69 | -127 |
| 592 | 774 | 2023-03-12T15:31:54.412Z | Ocean Networks Canada Society | 4.2 | 48.67 | -129.2 |
| 593 | 775 | 2023-03-19T14:45:26.895Z | Ocean Networks Canada Society | 3.4 | 49.55 | -127.43 |
| 603 | 788 | 2023-04-13T15:54:59.809Z | Ocean Networks Canada Society | 5.1 | 49.08 | -129.35 |
| 608 | 795 | 2023-04-19T18:56:24.023Z | Ocean Networks Canada Society | 4.6 | 48.59 | -130.29 |
| 607 | 794 | 2023-04-19T18:56:34.049Z | Ocean Networks Canada Society | 3.8 | 49.06 | -128.65 |
| 624 | 815 | 2023-07-07T09:12:37.312Z | Ocean Networks Canada Society | 3 | 48.34 | -123.02 |
| 626 | 820 | 2023-07-27T15:58:36.477Z | Ocean Networks Canada Society | 2.9 | 48.73 | -122.98 |
| 628 | 822 | 2023-08-08T10:17:38.092Z | Ocean Networks Canada Society | 3.2 | 48.08 | -123.03 |

| ID | Detailed Earthquake ID | Time | Organization | Magnitude | Latitude | Longitude |
|---|---|---|---|---|---|---|
| 630 | 824 | 2023-09-04T11:37:37.121Z | Ocean Networks Canada Society | 3.6 | 51 | -125.14 |
| 650 | 849 | 2023-09-28T12:33:31.612Z | Ocean Networks Canada Society | 3.2 | 49.44 | -126.82 |
| 657 | 861 | 2023-10-24T05:58:38.875Z | Ocean Networks Canada Society | 3.9 | 50.39 | -128.54 |
| 658 | 863 | 2023-11-17T00:47:39.797Z | Ocean Networks Canada Society | 3.5 | 48.18 | -122.39 |
| 663 | 868 | 2023-11-30T02:53:10.674Z | Ocean Networks Canada Society | 3.2 | 49.3 | -125.32 |
| 664 | 873 | 2023-12-17T23:23:14.410Z | Ocean Networks Canada Society | 4.4 | 51.15 | -124.32 |
| 665 | 874 | 2023-12-24T15:13:45.922Z | Ocean Networks Canada Society | 4.1 | 46.73 | -122.48 |
| 674 | 884 | 2024-01-16T22:24:03.408Z | Ocean Networks Canada Society | 3 | 48.41 | -124.84 |
| 676 | 888 | 2024-01-26T17:10:59.447Z | Ocean Networks Canada Society | 4 | 50.43 | -123.06 |
| 692 | 908 | 2024-02-24T05:53:45.362Z | Ocean Networks Canada Society | 3.4 | 49.36 | -127.96 |
| 717 | 936 | 2024-03-21T07:04:45.619Z | Ocean Networks Canada Society | 3 | 48.56 | -124.82 |
| 719 | 939 | 2024-03-22T08:57:16.755Z | Ocean Networks Canada Society | 3.2 | 49.75 | -127.03 |
| 722 | 944 | 2024-04-01T00:17:27.287Z | Ocean Networks Canada Society | 3.5 | 49.67 | -126.73 |
| 734 | 964 | 2024-05-03T03:03:32.531Z | Ocean Networks Canada Society | 4.1 | 48.81 | -128.74 |
| 739 | 969 | 2024-05-10T11:44:44.285Z | Ocean Networks Canada Society | 3.8 | 48.94 | -128.42 |
| 751 | 987 | 2024-07-04T16:15:09.462Z | Ocean Networks Canada Society | 4.6 | 48.75 | -128.57 |
| 759 | 1000 | 2024-07-05T02:09:12.448Z | Ocean Networks Canada Society | 3.3 | 49.16 | -127.72 |
| 761 | 1002 | 2024-07-05T15:51:52.687Z | Ocean Networks Canada Society | 4 | 48.73 | -128.38 |
| 762 | 1006 | 2024-07-05T16:34:07.524Z | Ocean Networks Canada Society | 4.2 | 48.69 | -128.49 |
| 768 | 1014 | 2024-07-06T11:01:07.316Z | Ocean Networks Canada Society | 3.8 | 48.54 | -128.47 |

| ID | Detailed Earthquake ID | Time | Organization | Magnitude | Latitude | Longitude |
|---|---|---|---|---|---|---|
| 770 | 1020 | 2024-07-08T15:06:52.151Z | Ocean Networks Canada Society | 3.6 | 48.94 | -128.36 |
| 771 | 1022 | 2024-07-08T17:06:02.691Z | Ocean Networks Canada Society | 3.9 | 48.72 | -128.49 |
| 774 | 1028 | 2024-07-11T15:08:50.692Z | Ocean Networks Canada Society | 5.3 | 48.73 | -128.82 |
| 775 | 1031 | 2024-07-11T16:17:21.970Z | Ocean Networks Canada Society | 4.4 | 48.93 | -128.64 |
| 776 | 1034 | 2024-07-11T17:34:29.796Z | Ocean Networks Canada Society | 3.7 | 48.88 | -128.66 |
| 780 | 1041 | 2024-07-12T08:20:06.718Z | Ocean Networks Canada Society | 4 | 48.37 | -123.78 |
| 779 | 1040 | 2024-07-12T08:20:30.513Z | Ocean Networks Canada Society | 4.2 | 48.86 | -128.79 |
| 792 | 1055 | 2024-07-15T21:09:42.785Z | Ocean Networks Canada Society | 3.8 | 49.81 | -123.55 |
| 803 | 1072 | 2024-07-23T16:12:22.554Z | Ocean Networks Canada Society | 3.9 | 50.26 | -129.09 |
| 805 | 1076 | 2024-08-02T08:19:31.238Z | Ocean Networks Canada Society | 3.7 | 48.99 | -128.26 |
| 806 | 1079 | 2024-08-07T04:49:01.748Z | Ocean Networks Canada Society | 3.3 | 48.79 | -125.46 |
| 807 | 1080 | 2024-08-09T06:14:16.403Z | Ocean Networks Canada Society | 3.7 | 50.67 | -124.53 |
| 808 | 1082 | 2024-08-14T00:08:08.252Z | Ocean Networks Canada Society | 3.5 | 48.87 | -128.25 |
| 809 | 1083 | 2024-08-23T10:23:40.740Z | Ocean Networks Canada Society | 3.6 | 48.97 | -128.27 |
| 810 | 1085 | 2024-08-26T15:15:36.836Z | Ocean Networks Canada Society | 3.2 | 48.82 | -126.05 |
| 850 | 1134 | 2024-09-25T01:33:24.830Z | Ocean Networks Canada Society | 3.1 | 50.1 | -127.88 |
| 854 | 1140 | 2024-09-26T11:05:24.536Z | Ocean Networks Canada Society | 3.5 | 48.57 | -123.41 |
| 863 | 1150 | 2024-10-02T15:36:02.936Z | Ocean Networks Canada Society | 3.8 | 49.29 | -128.03 |
| 864 | 1153 | 2024-10-02T20:25:56.436Z | Ocean Networks Canada Society | 3.1 | 49.67 | -126.66 |
| 865 | 1157 | 2024-10-04T09:09:02.847Z | Ocean Networks Canada Society | 3.5 | 48.95 | -123.42 |

| ID | Detailed Earthquake ID | Time | Organization | Magnitude | Latitude | Longitude |
|---|---|---|---|---|---|---|
| 869 | 1163 | 2024-10-08T13:59:37.075Z | Ocean Networks Canada Society | 3.9 | 51.33 | -125.99 |
| 889 | 1186 | 2024-11-25T08:24:37.437Z | Ocean Networks Canada Society | 4.1 | 47.41 | -128.96 |
| 894 | 1191 | 2024-12-06T06:31:52.258Z | Ocean Networks Canada Society | 3.7 | 48.59 | -129.93 |
| 896 | 1195 | 2024-12-13T04:32:35.252Z | Ocean Networks Canada Society | 3.6 | 49.66 | -127.14 |
| 898 | 1197 | 2024-12-13T16:18:55.904Z | Ocean Networks Canada Society | 3.2 | 50.15 | -128.15 |
| 907 | 1208 | 2025-01-29T14:26:46.379Z | Ocean Networks Canada Society | 3.4 | 49.42 | -125.92 |
| 909 | 1210 | 2025-01-30T12:48:36.239Z | Ocean Networks Canada Society | 4.1 | 51.88 | -126.38 |
| 912 | 1216 | 2025-02-14T05:59:20.237Z | Ocean Networks Canada Society | 3.4 | 48.3 | -123.33 |
| 14 | 16 | 2022-02-22T14:26:04.533Z | United States Geological Survey | 4 | 49.2327 | -129.0681 |
| 22 | 26 | 2022-04-23T21:22:47.948Z | United States Geological Survey | 5.3 | 50.4725 | -129.6895 |
| 114 | 437 | 2022-05-05T03:38:10.239Z | United States Geological Survey | 4.1 | 48.5563 | -128.9545 |
| 121 | 185 | 2022-06-04T23:59:10.007Z | United States Geological Survey | 5.1 | 51.6137 | -131.4027 |
| 123 | 190 | 2022-06-13T17:34:43.012Z | United States Geological Survey | 4.6 | 50.9202 | -129.9414 |
| 160 | 230 | 2022-07-26T05:46:22.180Z | United States Geological Survey | 4.6 | 51.6872 | -131.1931 |
| 163 | 235 | 2022-08-08T07:38:56.410Z | United States Geological Survey | 4.6 | 48.9736 | -128.6522 |
| 173 | 745 | 2022-09-22T14:41:56.900Z | United States Geological Survey | 3.5 | 48.0465 | -124.715 |
| 334 | 436 | 2022-11-07T03:17:18.976Z | United States Geological Survey | 4.2 | 50.5461 | -129.6746 |
| 338 | 440 | 2022-11-26T03:50:17.627Z | United States Geological Survey | 4.9 | 49.2766 | -126.0994 |
| 341 | 444 | 2022-12-06T13:29:18.635Z | United States Geological Survey | 4.6 | 50.6979 | -130.1776 |
| 575 | 748 | 2022-12-28T08:06:54.980Z | United States Geological Survey | 3.8 | 47.8047 | -128.9084 |

| ID | Detailed Earthquake ID | Time | Organization | Magnitude | Latitude | Longitude |
|---|---|---|---|---|---|---|
| 344 | 747 | 2022-12-28T08:07:48.135Z | United States Geological Survey | 3.9 | 47.841 | -128.9125 |
| 576 | 749 | 2023-01-28T16:10:51.373Z | United States Geological Survey | 4 | 49.0299 | -128.4935 |
| 581 | 755 | 2023-02-17T06:55:48.570Z | United States Geological Survey | 4.6 | 50.4493 | -129.6833 |
| 583 | 762 | 2023-02-20T09:08:36.002Z | United States Geological Survey | 4.1 | 48.7357 | -128.9459 |
| 590 | 769 | 2023-03-08T10:04:26.472Z | United States Geological Survey | 4.3 | 50.2338 | -129.6069 |
| 592 | 773 | 2023-03-12T15:31:54.125Z | United States Geological Survey | 4.3 | 48.7572 | -129.6185 |
| 595 | 778 | 2023-04-02T01:08:33.443Z | United States Geological Survey | 4.6 | 50.2814 | -129.5775 |
| 603 | 790 | 2023-04-13T15:54:53.811Z | United States Geological Survey | 6 | 49.2147 | -129.6178 |
| 606 | 793 | 2023-04-14T15:49:05.314Z | United States Geological Survey | 4.2 | 48.7907 | -129.4095 |
| 607 | 797 | 2023-04-19T18:56:31.548Z | United States Geological Survey | 4.3 | 49.1534 | -128.8899 |
| 619 | 812 | 2023-06-20T04:12:48.148Z | United States Geological Survey | 4.1 | 50.6524 | -129.8081 |
| 624 | 818 | 2023-07-07T09:12:34.430Z | United States Geological Survey | 2.6 | 48.3498333 | -123.00383 |
| 634 | 855 | 2023-09-14T17:31:07.100Z | United States Geological Survey | 4.2 | 50.8821 | -130.1593 |
| 633 | 854 | 2023-09-14T17:41:28.291Z | United States Geological Survey | 4.3 | 50.808 | -130.3913 |
| 641 | 836 | 2023-09-17T09:59:00.179Z | United States Geological Survey | 4.5 | 50.9314 | -130.0672 |
| 640 | 835 | 2023-09-17T09:59:18.000Z | United States Geological Survey | 4.3 | 50.332 | -128.649 |
| 639 | 834 | 2023-09-17T11:28:11.184Z | United States Geological Survey | 5.5 | 50.8079 | -130.3341 |
| 642 | 840 | 2023-09-17T15:19:50.439Z | United States Geological Survey | 4.1 | 50.8343 | -130.3241 |
| 647 | 845 | 2023-09-25T13:31:51.857Z | United States Geological Survey | 4.1 | 47.7239 | -128.4548 |
| 697 | 916 | 2023-10-09T02:21:08.810Z | United States Geological Survey | 4.3 | 48.0328333 | -122.7065 |

| ID | Detailed Earthquake ID | Time | Organization | Magnitude | Latitude | Longitude |
|---|---|---|---|---|---|---|
| 652 | 862 | 2023-10-11T11:15:26.664Z | United States Geological Survey | 4.1 | 50.8404 | -130.2555 |
| 655 | 858 | 2023-10-16T03:13:54.592Z | United States Geological Survey | 4.8 | 50.7034 | -129.9371 |
| 656 | 860 | 2023-10-24T05:58:20.546Z | United States Geological Survey | 4.5 | 50.5657 | -130.1793 |
| 663 | 869 | 2023-11-30T02:53:10.850Z | United States Geological Survey | 2.4 | 49.2928333 | -125.2635 |
| 664 | 872 | 2023-12-17T23:23:15.663Z | United States Geological Survey | 4.7 | 51.0962 | -124.397 |
| 670 | 880 | 2024-01-09T01:41:28.313Z | United States Geological Survey | 4.3 | 50.8188 | -130.0585 |
| 673 | 883 | 2024-01-15T07:25:05.920Z | United States Geological Survey | 3.5 | 48.0041667 | -123.16667 |
| 674 | 886 | 2024-01-16T22:24:01.650Z | United States Geological Survey | 3.2 | 48.2365 | -124.948 |
| 676 | 890 | 2024-01-26T17:11:05.373Z | United States Geological Survey | 3.1 | 49.8614 | -123.6026 |
| 677 | 895 | 2024-01-30T06:23:20.709Z | United States Geological Survey | 4.1 | 50.7449 | -129.9122 |
| 680 | 894 | 2024-02-05T07:33:13.117Z | United States Geological Survey | 3.8 | 47.5308 | -129.0334 |
| 689 | 905 | 2024-02-16T16:30:18.830Z | United States Geological Survey | 3.4 | 47.5928333 | -123.092 |
| 693 | 911 | 2024-03-06T08:41:27.085Z | United States Geological Survey | 4.6 | 48.0534 | -129.0191 |
| 717 | 947 | 2024-03-21T07:04:44.302Z | United States Geological Survey | 2.4 | 48.645 | -124.8131 |
| 723 | 946 | 2024-04-07T04:40:23.731Z | United States Geological Survey | 4.1 | 47.5038 | -129.0933 |
| 725 | 950 | 2024-04-17T21:46:14.392Z | United States Geological Survey | 4.9 | 50.1941 | -129.9152 |
| 726 | 952 | 2024-04-18T06:06:04.781Z | United States Geological Survey | 4.9 | 50.244 | -129.9458 |
| 727 | 957 | 2024-04-18T06:41:45.795Z | United States Geological Survey | 4.3 | 50.2149 | -129.8884 |
| 730 | 956 | 2024-04-18T08:40:12.653Z | United States Geological Survey | 4.1 | 50.3512 | -129.9026 |
| 734 | 963 | 2024-05-03T03:03:29.265Z | United States Geological Survey | 5 | 48.7813 | -128.7101 |

| ID | Detailed Earthquake ID | Time | Organization | Magnitude | Latitude | Longitude |
|---|---|---|---|---|---|---|
| 739 | 971 | 2024-05-10T11:44:38.834Z | United States Geological Survey | 4.3 | 48.8021 | -128.7697 |
| 743 | 976 | 2024-07-03T19:59:15.702Z | United States Geological Survey | 4.4 | 48.4888 | -128.7569 |
| 744 | 1047 | 2024-07-03T20:13:24.684Z | United States Geological Survey | 4.2 | 48.74 | -128.5301 |
| 786 | 1049 | 2024-07-03T20:16:50.426Z | United States Geological Survey | 4.4 | 48.326 | -128.9085 |
| 748 | 981 | 2024-07-03T20:18:13.474Z | United States Geological Survey | 4.6 | 48.4906 | -129.3694 |
| 790 | 1053 | 2024-07-03T20:18:13.474Z | United States Geological Survey | 4.6 | 48.4906 | -129.3694 |
| 789 | 1052 | 2024-07-03T20:19:35.973Z | United States Geological Survey | 4.5 | 48.4656 | -129.0821 |
| 747 | 980 | 2024-07-03T20:21:42.302Z | United States Geological Survey | 4.3 | 48.5794 | -128.7066 |
| 746 | 979 | 2024-07-03T20:23:46.026Z | United States Geological Survey | 4.3 | 48.5928 | -128.6725 |
| 769 | 1015 | 2024-07-03T20:25:13.237Z | United States Geological Survey | 4.9 | 48.5091 | -128.8575 |
| 745 | 978 | 2024-07-03T21:14:22.750Z | United States Geological Survey | 4.1 | 48.5007 | -128.6621 |
| 749 | 982 | 2024-07-04T05:01:23.413Z | United States Geological Survey | 4.2 | 48.4637 | -128.8203 |
| 750 | 984 | 2024-07-04T13:18:03.615Z | United States Geological Survey | 4.7 | 48.6735 | -129.1863 |
| 753 | 989 | 2024-07-04T16:00:18.332Z | United States Geological Survey | 4.2 | 48.7176 | -129.0315 |
| 751 | 986 | 2024-07-04T16:15:08.888Z | United States Geological Survey | 5.7 | 48.6536 | -129.0074 |
| 754 | 993 | 2024-07-04T17:43:18.003Z | United States Geological Survey | 4.3 | 48.6965 | -129.0814 |
| 755 | 995 | 2024-07-04T18:31:25.054Z | United States Geological Survey | 4.8 | 48.7389 | -129.0135 |
| 758 | 999 | 2024-07-04T21:20:20.355Z | United States Geological Survey | 4.4 | 48.4607 | -128.9043 |
| 764 | 1017 | 2024-07-04T23:13:29.156Z | United States Geological Survey | 4.3 | 48.5197 | -128.7902 |
| 766 | 1061 | 2024-07-05T01:48:43.127Z | United States Geological Survey | 4.4 | 48.5998 | -128.8591 |

| ID | Detailed Earthquake ID | Time | Organization | Magnitude | Latitude | Longitude |
|---|---|---|---|---|---|---|
| 763 | 1062 | 2024-07-05T02:09:01.963Z | United States Geological Survey | 4.3 | 48.5769 | -128.9508 |
| 760 | 1001 | 2024-07-05T09:05:13.394Z | United States Geological Survey | 4 | 48.6856 | -128.7357 |
| 762 | 1005 | 2024-07-05T16:34:05.014Z | United States Geological Survey | 5.3 | 48.6174 | -129.0585 |
| 768 | 1016 | 2024-07-06T11:01:06.526Z | United States Geological Survey | 4.2 | 48.3258 | -128.9731 |
| 770 | 1019 | 2024-07-08T15:06:44.416Z | United States Geological Survey | 5.2 | 48.671 | -128.9811 |
| 771 | 1075 | 2024-07-08T17:05:53.842Z | United States Geological Survey | 4.4 | 48.6368 | -128.8617 |
| 774 | 1027 | 2024-07-11T15:08:47.040Z | United States Geological Survey | 6.4 | 48.7668 | -128.7197 |
| 802 | 1069 | 2024-07-11T15:17:35.633Z | United States Geological Survey | 4.5 | 48.8019 | -128.7385 |
| 773 | 1068 | 2024-07-11T15:35:41.801Z | United States Geological Survey | 4.2 | 48.932 | -128.7769 |
| 775 | 1030 | 2024-07-11T16:17:20.281Z | United States Geological Survey | 5.2 | 48.8616 | -128.6109 |
| 776 | 1035 | 2024-07-11T17:34:26.968Z | United States Geological Survey | 4.7 | 48.7663 | -128.693 |
| 779 | 1039 | 2024-07-12T08:20:30.586Z | United States Geological Survey | 4.8 | 49.0384 | -128.3628 |
| 785 | 1046 | 2024-07-14T02:25:17.751Z | United States Geological Survey | 4.4 | 48.8962 | -128.7941 |
| 792 | 1102 | 2024-07-15T21:09:38.692Z | United States Geological Survey | 2.6 | 49.8325 | -123.5992 |
| 803 | 1073 | 2024-07-23T16:12:14.615Z | United States Geological Survey | 4.4 | 50.6244 | -129.8113 |
| 805 | 1077 | 2024-08-02T08:19:25.081Z | United States Geological Survey | 4.1 | 48.6527 | -128.7874 |
| 806 | 1105 | 2024-08-07T04:49:03.770Z | United States Geological Survey | 2.6 | 48.705 | -125.5465 |
| 817 | 1162 | 2024-09-15T21:39:52.692Z | United States Geological Survey | 4 | 51.7148 | -130.6856 |
| 813 | 1089 | 2024-09-15T22:22:48.323Z | United States Geological Survey | 6.5 | 51.5827 | -130.6302 |
| 814 | 1166 | 2024-09-15T23:26:47.109Z | United States Geological Survey | 4 | 51.5327 | -130.6439 |

| ID | Detailed Earthquake ID | Time | Organization | Magnitude | Latitude | Longitude |
|---|---|---|---|---|---|---|
| 816 | 1092 | 2024-09-16T01:43:25.399Z | United States Geological Survey | 4.7 | 51.3822 | -130.8184 |
| 828 | 1110 | 2024-09-18T12:02:12.490Z | United States Geological Survey | 4.2 | 51.5621 | -130.6399 |
| 854 | 1139 | 2024-09-26T11:05:20.170Z | United States Geological Survey | 4 | 48.5806667 | -123.24783 |
| 863 | 1151 | 2024-10-02T15:35:51.599Z | United States Geological Survey | 4.1 | 49.2368 | -128.9843 |
| 865 | 1158 | 2024-10-04T09:08:58.475Z | United States Geological Survey | 3.6 | 49.0484 | -123.4017 |
| 889 | 1185 | 2024-11-25T08:24:36.716Z | United States Geological Survey | 4.6 | 47.565 | -128.8924 |
| 894 | 1193 | 2024-12-06T06:32:02.434Z | United States Geological Survey | 4.1 | 49.12 | -128.9882 |
| 900 | 1200 | 2024-12-25T21:39:29.258Z | United States Geological Survey | 5 | 50.5968 | -130.2621 |
| 906 | 1207 | 2025-01-29T13:53:36.056Z | United States Geological Survey | 4.2 | 47.8167 | -128.2878 |
| 910 | 1213 | 2025-02-03T00:25:36.386Z | United States Geological Survey | 4.4 | 51.5203 | -130.8978 |
| 911 | 1215 | 2025-02-06T12:05:48.914Z | United States Geological Survey | 4 | 50.4967 | -130.053 |
| 912 | 1218 | 2025-02-14T05:59:18.270Z | United States Geological Survey | 3.7 | 48.2913333 | -123.27933 |

# Appendix B

| ID | Magnitude | Latitude | Longitude |
|---|---|---|---|
| 10 | 3.8 | 50.0158 | -128.3562 |
| 11 | 3.6 | 48.4875 | -128.72 |
| 12 | 3.5 | 50.6508 | -130.5788 |
| 13 | 3.6 | 48.0726 | -129.0415 |
| 14 | 3.9 | 48.8558 | -129.491 |
| 16 | 3.8 | 50.4768 | -130.1544 |
| 19 | 3.7 | 51.2837 | -130.8967 |
| 20 | 3.7 | 51.3529 | -130.7868 |
| 25 | 3.7 | 50.2791 | -129.941 |
| 114 | 4.1 | 48.5661 | -128.9165 |
| 115 | 3.5 | 48.553 | -128.9276 |
| 116 | 3.6 | 46.9375 | -129.1609 |
| 118 | 3.7 | 50.4043 | -130.2942 |
| 119 | 3.5 | 47.6099 | -129.1517 |
| 120 | 3.7 | 51.6105 | -131.421 |
| 121 | 5.1 | 51.6219 | -131.4151 |
| 123 | 4.6 | 50.6509 | -130.5102 |
| 124 | 3.7 | 48.7233 | -129.0068 |

| | | | |
|---|---|---|---|
| 158 | 3.5 | 47.5652 | -129.0251 |
| 160 | 4.8 | 51.6133 | -131.3443 |
| 161 | 3.7 | 51.5972 | -131.3987 |
| 162 | 3.6 | 51.611 | -131.409 |
| 164 | 3.6 | 50.9883 | -130.6432 |
| 165 | 3.6 | 48.7387 | -129.1791 |
| 166 | 3.6 | 49.7256 | -130.5257 |
| 169 | 3.6 | 50.6971 | -130.5951 |
| 174 | 3.8 | 47.5718 | -129.0669 |
| 175 | 3.8 | 50.5152 | -130.3024 |
| 176 | 3.8 | 51.3401 | -131.409 |
| 177 | 3.5 | 48.33 | -128.9525 |
| 335 | 3.5 | 51.6246 | -131.0772 |
| 336 | 3.7 | 50.9819 | -130.6462 |
| 337 | 4 | 47.6776 | -129.1875 |
| 339 | 3.5 | 50.6677 | -130.5554 |
| 340 | 3.9 | 50.4482 | -130.2823 |
| 342 | 5.2 | 50.5278 | -130.4713 |
| 343 | 3.9 | 48.8686 | -129.8747 |
| 344 | 4.2 | 47.6532 | -129.1574 |
| 345 | 4.1 | 47.6796 | -129.1949 |

| | | | |
|---|---|---|---|
| 346 | 3.5 | 48.9231 | -129.8607 |
| 574 | 3.7 | 49.7232 | -130.8693 |
| 577 | 4.2 | 50.0407 | -130.0408 |
| 578 | 3.8 | 48.8816 | -128.5886 |
| 579 | 3.7 | 51.3052 | -131.0023 |
| 580 | 3.9 | 48.8227 | -129.2656 |
| 581 | 4.8 | 50.2126 | -129.7826 |
| 582 | 3.7 | 50.8002 | -130.6122 |
| 586 | 3.9 | 50.4674 | -130.288 |
| 587 | 3.7 | 50.1016 | -129.6658 |
| 588 | 3.9 | 50.0978 | -129.6536 |
| 589 | 3.5 | 48.05 | -128.5325 |
| 590 | 4.1 | 50.07 | -129.6012 |
| 591 | 4 | 50.0715 | -129.6946 |
| 594 | 4 | 50.5366 | -130.2837 |
| 595 | 4.5 | 50.0813 | -129.7193 |
| 596 | 3.7 | 50.5644 | -130.4382 |
| 597 | 3.8 | 49.9895 | -130.1096 |
| 598 | 3.6 | 50.5295 | -130.3151 |
| 599 | 3.7 | 50.8288 | -130.5676 |
| 600 | 3.8 | 48.2936 | -129.0441 |

| | | | |
|---|---|---|---|
| 601 | 3.7 | 50.095 | -129.5898 |
| 602 | 3.8 | 50.1303 | -129.652 |
| 604 | 4.3 | 49.0511 | -129.8315 |
| 605 | 3.5 | 49.0815 | -129.7877 |
| 606 | 4 | 48.7829 | -129.2676 |
| 609 | 4.1 | 47.5907 | -129.1071 |
| 610 | 3.6 | 48.7736 | -129.2484 |
| 611 | 3.7 | 51.2846 | -130.7964 |
| 612 | 3.7 | 50.5776 | -130.3619 |
| 613 | 3.6 | 50.5622 | -130.3422 |
| 614 | 3.7 | 50.5203 | -130.255 |
| 615 | 3.7 | 49.1282 | -130.1786 |
| 616 | 3.7 | 47.9848 | -128.2561 |
| 617 | 4 | 50.463 | -130.2613 |
| 618 | 4.1 | 50.4896 | -130.4148 |
| 619 | 4.3 | 50.3943 | -130.2594 |
| 620 | 3.7 | 50.4504 | -130.1601 |
| 621 | 3.6 | 50.4622 | -130.1747 |
| 622 | 3.9 | 50.4416 | -130.2614 |
| 623 | 3.8 | 50.2094 | -130.215 |
| 625 | 3.7 | 50.7151 | -130.5214 |

| | | | |
|---|---|---|---|
| 627 | 3.6 | 50.7023 | -130.5351 |
| 629 | 3.6 | 50.7357 | -130.5014 |
| 631 | 4 | 50.6497 | -130.4835 |
| 632 | 4.1 | 50.6614 | -130.5134 |
| 633 | 4.3 | 50.6413 | -130.4797 |
| 634 | 4.2 | 50.6583 | -130.4471 |
| 635 | 3.9 | 50.6256 | -130.5323 |
| 636 | 4 | 50.6608 | -130.4568 |
| 637 | 3.7 | 50.6303 | -130.4872 |
| 638 | 3.7 | 50.6817 | -130.4249 |
| 639 | 5.4 | 50.6079 | -130.533 |
| 641 | 4.5 | 50.609 | -130.4833 |
| 642 | 4.4 | 50.652 | -130.4561 |
| 643 | 4 | 50.577 | -130.4968 |
| 644 | 4 | 50.6392 | -130.4832 |
| 645 | 3.5 | 50.6121 | -130.4655 |
| 646 | 3.7 | 50.693 | -130.436 |
| 647 | 4.1 | 47.4262 | -128.8975 |
| 648 | 4.1 | 47.511 | -129.2241 |
| 649 | 3.7 | 50.7074 | -130.48 |
| 651 | 3.6 | 50.6974 | -130.3777 |

| | | | |
|---|---|---|---|
| 652 | 4.3 | 50.5636 | -130.5084 |
| 653 | 3.9 | 51.2373 | -130.78 |
| 654 | 3.5 | 48.6603 | -128.4509 |
| 655 | 4.9 | 50.5334 | -130.3604 |
| 656 | 4.6 | 50.4749 | -130.2889 |
| 659 | 3.7 | 47.3998 | -129.1986 |
| 660 | 3.8 | 49.12 | -129.3202 |
| 661 | 3.5 | 50.3439 | -130.122 |
| 662 | 3.6 | 48.7568 | -129.1592 |
| 666 | 3.8 | 50.5408 | -130.2707 |
| 667 | 3.9 | 50.4875 | -130.1551 |
| 668 | 3.5 | 48.7929 | -129.0699 |
| 669 | 3.6 | 50.5693 | -130.3243 |
| 670 | 4.8 | 50.6373 | -130.4279 |
| 671 | 3.5 | 50.1956 | -129.6316 |
| 672 | 3.7 | 50.7157 | -130.4299 |
| 675 | 3.6 | 50.5696 | -130.2401 |
| 677 | 4.5 | 50.5343 | -130.3549 |
| 678 | 3.7 | 51.2541 | -130.9406 |
| 679 | 3.8 | 48.4227 | -127.7039 |
| 680 | 3.9 | 47.5098 | -129.1513 |

| | | | |
|---|---|---|---|
| 681 | 3.7 | 50.7081 | -130.4342 |
| 682 | 3.6 | 50.7001 | -130.4204 |
| 683 | 3.7 | 47.5615 | -128.904 |
| 684 | 3.7 | 47.6006 | -129.079 |
| 685 | 3.8 | 47.5003 | -129.2674 |
| 686 | 3.7 | 47.6035 | -129.1073 |
| 687 | 3.5 | 47.2335 | -128.5787 |
| 688 | 3.6 | 51.4697 | -131.2703 |
| 690 | 3.6 | 51.145 | -131.1085 |
| 691 | 3.6 | 50.5832 | -130.3739 |
| 693 | 4.6 | 48.0459 | -129.0248 |
| 694 | 3.7 | 49.3324 | -129.9361 |
| 695 | 3.7 | 48.0078 | -128.9815 |
| 696 | 3.6 | 48.0662 | -129.0604 |
| 697 | 4 | 48.0385 | -122.7547 |
| 698 | 3.7 | 49.1288 | -128.0463 |
| 699 | 3.6 | 48.4601 | -128.2342 |
| 700 | 3.9 | 48.7388 | -129.6597 |
| 701 | 3.9 | 48.725 | -129.6995 |
| 702 | 3.6 | 48.752 | -129.6702 |
| 703 | 4.2 | 48.7335 | -129.6976 |

| | | | |
|---|---|---|---|
| 704 | 4.2 | 48.7146 | -129.7546 |
| 705 | 3.6 | 48.6924 | -129.1615 |
| 706 | 3.8 | 48.6692 | -129.0972 |
| 707 | 3.8 | 48.7127 | -129.7639 |
| 708 | 3.9 | 48.6625 | -129.082 |
| 709 | 3.8 | 48.7148 | -129.6812 |
| 710 | 4.2 | 48.7238 | -129.7282 |
| 711 | 3.6 | 48.6796 | -129.0377 |
| 712 | 3.7 | 48.8324 | -128.6497 |
| 713 | 3.6 | 48.6574 | -129.0592 |
| 714 | 3.8 | 48.7391 | -129.0082 |
| 715 | 3.6 | 48.6982 | -128.9491 |
| 716 | 3.6 | 48.7457 | -128.9947 |
| 718 | 3.7 | 48.7087 | -129.044 |
| 720 | 3.6 | 50.7882 | -130.5103 |
| 721 | 3.6 | 48.7205 | -128.9805 |
| 725 | 4.9 | 49.9959 | -130.0883 |
| 726 | 4.8 | 50.0007 | -130.1785 |
| 727 | 4.4 | 49.9391 | -130.1767 |
| 728 | 3.8 | 50.0405 | -130.2452 |
| 729 | 3.5 | 49.96 | -130.1644 |

| | | | |
|---|---|---|---|
| 730 | 3.8 | 50.0487 | -130.1936 |
| 731 | 3.6 | 49.9929 | -130.216 |
| 732 | 3.6 | 48.732 | -128.8639 |
| 733 | 3.6 | 49.3726 | -130.2915 |
| 735 | 3.5 | 48.7614 | -128.8122 |
| 736 | 3.6 | 48.7672 | -128.82 |
| 737 | 3.5 | 48.7643 | -128.8239 |
| 738 | 3.6 | 48.7273 | -128.7774 |
| 740 | 3.6 | 47.5531 | -129.2761 |
| 741 | 3.9 | 50.5574 | -130.4222 |
| 742 | 3.8 | 50.7378 | -130.5986 |
| 743 | 3.9 | 48.2346 | -129.0432 |
| 744 | 4.1 | 48.1386 | -129.007 |
| 749 | 3.6 | 48.5198 | -128.9124 |
| 750 | 4.9 | 48.6917 | -129.2656 |
| 753 | 4.4 | 48.6645 | -129.0635 |
| 754 | 4.4 | 48.6987 | -129.1115 |
| 755 | 4.7 | 48.7307 | -129.1616 |
| 756 | 3.6 | 48.724 | -129.1254 |
| 757 | 3.6 | 48.6135 | -129.0588 |
| 758 | 3.7 | 48.5625 | -128.9081 |

| | | | |
|---|---|---|---|
| 763 | 4.5 | 48.6843 | -129.0421 |
| 764 | 3.7 | 48.5228 | -128.8717 |
| 765 | 3.7 | 48.7508 | -129.1477 |
| 766 | 3.6 | 48.5212 | -128.8768 |
| 767 | 3.5 | 48.5394 | -128.9343 |
| 772 | 3.5 | 48.7612 | -129.0847 |
| 773 | 4 | 48.8532 | -128.6748 |
| 777 | 3.6 | 48.6363 | -128.6512 |
| 778 | 3.7 | 48.8449 | -128.6138 |
| 781 | 3.8 | 48.7128 | -128.9533 |
| 782 | 3.6 | 48.871 | -128.7205 |
| 783 | 3.7 | 48.6924 | -128.8444 |
| 785 | 4.1 | 48.8778 | -128.7634 |
| 787 | 3.7 | 48.856 | -128.6652 |
| 788 | 3.6 | 48.8676 | -128.6669 |
| 791 | 3.8 | 48.8627 | -128.6954 |
| 793 | 3.7 | 48.862 | -128.745 |
| 794 | 3.6 | 48.8716 | -128.7289 |
| 795 | 3.5 | 48.8924 | -128.6503 |
| 796 | 3.6 | 48.8526 | -128.625 |
| 797 | 3.8 | 50.4058 | -130.2253 |

| | | | |
|---|---|---|---|
| 798 | 3.8 | 48.8605 | -128.7701 |
| 799 | 3.6 | 48.923 | -128.5495 |
| 800 | 3.5 | 48.4997 | -128.8438 |
| 801 | 3.6 | 48.8244 | -128.6421 |
| 802 | 4.1 | 48.8119 | -128.649 |
| 804 | 3.5 | 50.449 | -130.2106 |
| 811 | 3.6 | 48.6334 | -128.8528 |
| 812 | 3.5 | 50.9784 | -130.71 |
| 813 | 6.5 | 51.3643 | -130.9513 |
| 814 | 4.5 | 51.3648 | -130.8723 |
| 816 | 4.8 | 51.359 | -130.8154 |
| 817 | 4.5 | 51.5439 | -130.7515 |
| 818 | 4.5 | 51.2583 | -130.7789 |
| 819 | 4.6 | 51.2731 | -130.8374 |
| 820 | 4.3 | 51.4944 | -130.9977 |
| 821 | 4.3 | 51.5731 | -130.8485 |
| 822 | 3.8 | 51.5092 | -130.9854 |
| 823 | 3.8 | 51.3122 | -130.682 |
| 824 | 3.6 | 51.3701 | -130.7152 |
| 825 | 4.4 | 51.2668 | -130.7499 |
| 826 | 4.2 | 51.511 | -130.918 |

| | | | |
|---|---|---|---|
| 827 | 4.1 | 51.6045 | -130.869 |
| 828 | 4.7 | 51.3016 | -130.8575 |
| 829 | 4.1 | 51.3691 | -131.027 |
| 830 | 4.1 | 51.3941 | -130.6585 |
| 831 | 3.6 | 51.538 | -130.8427 |
| 832 | 4.5 | 51.3304 | -130.8548 |
| 833 | 4.3 | 51.1945 | -130.7934 |
| 834 | 3.7 | 51.4621 | -130.9567 |
| 835 | 3.9 | 51.2822 | -130.7744 |
| 836 | 4 | 51.5225 | -130.8261 |
| 837 | 4.3 | 51.2081 | -130.8228 |
| 838 | 4.2 | 51.0211 | -130.6851 |
| 839 | 4.2 | 51.5669 | -130.7614 |
| 840 | 4 | 51.5679 | -130.8931 |
| 841 | 4 | 51.5076 | -130.8382 |
| 842 | 4 | 51.3769 | -130.8555 |
| 843 | 4 | 51.4719 | -130.8959 |
| 844 | 3.6 | 51.5406 | -130.8757 |
| 845 | 3.8 | 51.3352 | -130.7748 |
| 846 | 3.6 | 51.4076 | -130.8755 |
| 847 | 3.6 | 51.5123 | -130.9311 |

| | | | |
|---|---|---|---|
| 848 | 3.5 | 51.2923 | -130.9281 |
| 849 | 4.1 | 51.3585 | -130.9116 |
| 851 | 4 | 51.3712 | -130.8606 |
| 852 | 3.8 | 51.5559 | -130.88 |
| 853 | 3.8 | 51.3554 | -130.8059 |
| 855 | 3.7 | 51.4602 | -130.8828 |
| 856 | 3.8 | 51.441 | -130.9079 |
| 857 | 4.3 | 51.4548 | -130.8698 |
| 858 | 3.8 | 51.558 | -130.8688 |
| 859 | 4 | 51.5602 | -130.7991 |
| 860 | 3.7 | 51.608 | -130.748 |
| 861 | 3.9 | 51.4969 | -130.973 |
| 862 | 3.6 | 51.4935 | -130.8722 |
| 866 | 4.1 | 51.4983 | -130.8246 |
| 867 | 3.7 | 51.4784 | -130.853 |
| 868 | 3.7 | 51.4687 | -130.9216 |
| 870 | 3.6 | 50.2875 | -129.9101 |
| 871 | 3.6 | 49.2505 | -128.5362 |
| 872 | 3.6 | 51.5315 | -130.8195 |
| 873 | 3.7 | 48.8472 | -129.0502 |
| 874 | 3.6 | 51.3847 | -130.8574 |

| | | | |
|---|---|---|---|
| 875 | 3.6 | 48.7423 | -128.7578 |